Fall 1-31-1998

Low pressure chemical vapor deposition of boron nitride thin films from triethylamine borane complex and ammonia

Narahari Ramanuja
New Jersey Institute of Technology

Copyright Warning & Restrictions

The copyright law of the United States (Title 17, United States Code) governs the making of photocopies or other reproductions of copyrighted material.

Under certain conditions specified in the law, libraries and archives are authorized to furnish a photocopy or other reproduction. One of these specified conditions is that the photocopy or reproduction is not to be "used for any purpose other than private study, scholarship, or research." If a, user makes a request for, or later uses, a photocopy or reproduction for purposes in excess of "fair use" that user may be liable for copyright infringement,

This institution reserves the right to refuse to accept a copying order if, in its judgment, fulfillment of the order would involve violation of copyright law.

Please Note: The author retains the copyright while the New Jersey Institute of Technology reserves the right to distribute this thesis or dissertation

Printing note: If you do not wish to print this page, then select "Pages from: first page # to: last page #" on the print dialog screen

ABSTRACT

LOW PRESSURE CHEMICAL VAPOR DEPOSITION OF BORON NITRIDE THIN FILMS FROM TRIETHYLAMINE BORANE COMPLEX AND AMMONIA

by
Narahari Ramanuja

Boron nitride thin films were synthesized on Silicon and quartz substrates by low pressure chemical vapor deposition using triethylamine-borane complex and ammonia as precursors. The films were processed at 550°C, 575°C and 600°C at a constant pressure of 0.05 Torr at different precursor flow rates and flow ratios.

Several analytical methods such as Fourier transform infrared spectroscopy, x- ray photo-electron spectroscopy, ultra-violet/visible spectrophotometry, ellipsometry, surface profilometry and scanning electron microscopy were used to study the deposited films. The films deposited were uniform, amorphous and the composition of the films varied with deposition temperature and precursor flow ratios. The stresses in the film were either mildly tensile or compressive.

Dielectric constant characterization of LPCVD boron nitride was made using metal-insulator-semiconductor (MIS) and metal-insulator-metal (MIM) structures. The boron nitride films were stable and showed dielectric constant values between 3.8 and 4.7. The limitation of attaining lower values could be due to the presence of carbon as an impurity in the film and the presence of mobile charge carriers in the films as well as at the substrate-film interface.

LOW PRESSURE CHEMICAL VAPOR DEPOSITION OF BORON NITRIDE THIN FILMS FROM TRIETHYLAMINE BORANE COMPLEX AND AMMONIA

by
Narahari Ramanuja

A Thesis
Submitted to the faculty of
New Jersey Institute of Technology
in Partial Fulfillment of the Requirements for the Degree of
Master of Science in Materials Science and Engineering

Department of Materials Science and Engineering

January 1998

APPROVAL PAGE

LOW PRESSURE CHEMICAL VAPOR DEPOSITION OF BORON NITRIDE THIN FILMS FROM TRIETHYLAMINE BORANE COMPLEX AND AMMONIA

Narahari Ramanuja

Dr. Roland A. Levy, Thesis Advisor — Date
Distinguished Professor of Physics, NJIT

Dr. John F. Federici, Committee Member, — Date
Professor of Physics, NJIT

Dr. Durga Misra, Committee Member, — Date
Associate Professor of Electrical and Computer Engineering, NJIT

BIOGRAPHICAL SKETCH

Author: Narahari Ramanuja

Degree: Master of Science

Date: January 1998

Undergraduate and Graduate Education:

- Master of Science in Materials Science and Engineering,
  New Jersey Institute of Technology,
  Newark, NJ, 1998

- Bachelor of Engineering in Chemical Engineering,
  Rashtreeya Vidyalaya College of Engineering (R. V. C. E),
  Bangalore University,
  Bangalore, India, 1996

Presentations:

R. A. Levy, N. Ramanuja, and L. N. Krasnoperov, " Design and Characterization of Ceramic Membrane Modules for VOC Separation." Presented in New Jersey Institute of Technology, Newark, New Jersey, October 1997, at the Hazardous Substance Management Research Center.

R. A. Levy, N. Ramanuja, " Multi-Lifecycle Engineering of CRT Glass" Presented in New Jersey Institute of Technology, Newark, New Jersey, July 1997, at the Multi-Lifecycle Engineering Research Center.

This thesis is dedicated to
my dear parents

ACKNOWLEDGMENT

I would like to express my sincere gratitude to my advisor, Professor Roland A. Levy for his guidance, inspiration, and support throughout this research.

Special thanks to Professor Durga Misra and Professor John F.Federici for serving as members of the thesis review committee.

I would like to thank Dr. Oktay Gokce and Dr. Pradyumna K. Swain for their help and guidance. I would also like to thank the CVD lab members including, Dr. Romiana Petrova, Vitaly Sigal, Krit Aryusook, Ravindranath Chenna and Kiran Kumar for their help and encouragement.

TABLE OF CONTENTS

TABLE OF CONTENTS
(Continued)

TABLE OF CONTENTS
(Continued)

TABLE OF CONTENTS
(Continued)

LIST OF TABLES

LIST OF FIGURES

LIST OF FIGURES
(Continued)

CHAPTER 1

INTRODUCTION

Boron nitride is a high resistivity semiconductor with a large bandgap. It is one of the most interesting materials of the III-V compounds having properties such as multiband electro-, photo-, and cathode-ray luminescence [1], electrically insulating, chemically inert, thermally stable, resistant to corrosion, and having desirable mechanical properties. Potential applications of boron nitride films include using the boron nitride film as high temperature dielectric [2], heat-dissipation coatings [3], passivation layers [1], diffusion sources of boron [4], and sodium barrier [1]. Since boron nitride is highly transparent to x-rays, it can be used in the fabrication of masks for x-ray lithography [5]. Also, the lubricative characteristics of its laminar structure make it a uniquely qualified material for fiber coatings in ceramic matrix composites (CMC) [6].

Since the creation of the first integrated circuit in 1960, there has been an ever-increasing density of devices manufacturable on semiconductor substrates. Integrated circuit dimensions will continue to shrink until a 0.03-μm minimum feature size is reached sometime in the second decade of the twenty-first century [7]. To attain these standards research has to be done primarily in three fields which include replacing the existing interconnect materials, replacing the SiO_2 based insulators as interlayer dielectrics (ILDs) with lower dielectric constant materials or changing the metallization schemes by implementing multi level metallization. [8]

IBM has already announced that it has developed a new semiconductor manufacturing process to shrink electronic circuitry to smaller dimensions and fit more computer logic, or "intelligence," on to a single chip. This technology, called CMOS 7S, is the first to use copper instead of aluminum to create the circuitry on silicon wafers. Integrating six layers of metal on a chip, CMOS 7S is the first process technology to use a production copper metallization process. The most desirable properties for the interlayer dielectric materials include low dielectric constant, low mechanical stress, high thermal stability and low moisture absorption.

One of the most promising inorganic dielectric materials is CVD boron nitride film. A number of synthetic routes have been developed for producing boron nitride. These include classical high–temperature routes and vapor deposition routes. The primary aim of the present work is to:

- Fabricate boron nitride thin films by low pressure chemical vapor deposition
- Characterize these films
- Optimize deposition parameters to obtain low stress and low dielectric constant films

Chemical vapor deposition is one of the methods of fabricating boron nitride thin films. The process, its positive and negative points and the salient features of the process are described in the subsequent sections. Further, the properties of dielectric materials and their applications in very large scale integrated (VLSI) technology is discussed.

In Chapter 2, a review of literature of boron nitride thin films, the preparation techniques and the influence of microstructure of boron nitride thin films on the properties are discussed. In addition, an overview of low dielectric constant materials in

general, and BN, SiBN and B-N-F ternary thin films as low dielectric constant materials in particular, are discussed.

In Chapter 3, the experimental procedure to fabricate boron nitride films and the characterization techniques used are described.

The important results of this work are described in Chapter 4 and the effect of various deposition parameters on the properties is discussed in detail.

Concluding remarks and suggestions for future work are given in Chapter 5.

1.1 Thin-Film Deposition Methods

Thin-film deposition techniques have traditionally been used in the microelectronics industry for microchip coating, wear and corrosion resistance, and thermal protection. Deposition methods can be classified under two groups: Physical Vapor Deposition (PVD) and Chemical Vapor Deposition (CVD).

1.1.1 Physical Vapor Deposition

Physical vapor deposition (PVD) is mainly focused into two categories, evaporation and sputtering. The objective of these deposition techniques is to controllably transfer atoms from a source to a substrate where film formation and growth proceed atomistically, without the need of a chemical reaction.

In evaporation, atoms are removed from the source by thermal means, whereas in sputtering the atoms are dislodged from a solid target by the impact of gaseous ions. Advances in vacuum-pumping equipment and Joule heating sources spurred the emergence of PVD as a suitable industrial film deposition process. In general, the

properties of the film obtained by PVD are governed by the following: evaporation rate of the atoms, vapor pressure of the target materials, deposition geometry, temperature, pressure, and thermal history of the substrate[52].

Traditionally, evaporation was the preferred PVD technique over sputtering. Higher deposition rates, better vacuum (thus cleaner environments for film formation and growth), and versatility in the fact that all classes of materials can apply were some of the reasons for the dominance of evaporation. The microelectronics revolution required the use of alloys with strict stoichiometric limits, which had to conformally cover and adhere well to substrate surfaces. This facilitated the need for the sputtering technique and so, as developments were made in radio frequency, bias, and magnetron variants, so were advances made in sputtering. These variants extended the capabilities of sputtering, as did the availability of high purity targets and working gases. The decision to use either technique depends solely on the desired application and has even spurred the development of hybrid techniques[52]. A comparison of the two is given in Table 1.1.

Table 1.1 Evaporation vs. Sputtering

Evaporation	Sputtering
A. Production of Vapor Species	
1. Thermal evaporation mechanism	Ion bombardment and collisional momentum transfer
2. Low kinetic energy of evaporant atoms (@ 1200 K , E = 0.1 eV)	2. High kinetic energy of sputtered atoms (E = 2-30 eV)
3. Evaporation rate ~ 1.3 x 10^{17} atoms/cm^2-sec	3. Sputter rate ~ 3 x 10^{16} atoms/cm^2-sec
4. Directional evaporation according to cosine law	4. Directional sputtering according to cosine law at high sputter rates
5. Fractionation of multicomponent alloys, decomposition, and dissociation of compounds	5. Generally good maintenance of target stoichiometry, but some dissociation of compounds
6. Availability of high evaporation source purities	6. Sputter target of all materials are available; purity varies with material
A. The Gas Phase	
1. Evaporant atoms travel in high or ultrahigh vacuum (~ 10^{-6} - 10^{-10} torr) ambient	1. Sputtered atoms encounter high pressure discharge region (~ 100 mtorr)
2. Thermal velocity of evaporant 10^5 cm/sec	2. Neutral atom velocity ~ 5 x 10^4 cm/sec
3. Mean-free path is larger than evaporant-substrate spacing; evaporant atoms undergo no collisions in vacuum	3. Mean-free path is less than target-substrate spacing; Sputtered atoms undergo many collisions in the discharge
A. The Condensed Film	
1. Condensing atoms have relatively low energy	1. Condensing atoms have high energy
2. Low gas incorporation	2. Some gas incorporation
3. Grain size generally larger than for sputtered film	3. Good adhesion to substrate
4. Few grain orientations (textured films)	4. Many grain orientations

Chemical vapor deposition is discussed next. Some factors that distinguish PVD from CVD are:

1. Reliance on solid or molten sources
2. Physical mechanisms (evaporation or collisional impact) by which source atoms enter the gas phase
3. Reduced pressure environment through which the gaseous species are transported

General absence of chemical reactions in the gas phase and at the substrate surface (reactive PVD processes are exceptions).

1.1.2 Chemical Vapor Deposition: Chemical Vapor Deposition (CVD) is one of the most important methods of film formation used in the fabrication of very large scale integrated (VLSI) silicon circuits, as well as of microelectronic solid state devices in general. It may be defined as the formation of a non-volatile solid film on a substrate by the reaction of vapor phase chemicals (reactants) that contain the required constituents. In this process, chemicals in the gas or vapor phase are reacted at the surface of the substrate where they form a solid product. A large variety of materials, practically all those needed in microelectronic device technology, can be created by CVD. These materials comprise insulators and dielectrics, elemental and compound semiconductors, electrical conductors, superconductors and magnetics. In addition to its unique versatility, this materials synthesis and vapor phase growth method can operate efficiently at relatively low temperatures. For example, refractory oxide glasses and metals can be deposited at temperatures of only 300° to 500°C. This feature is very important in advanced VLSI devices with short channel lengths and shallow junctions, where lateral and vertical

diffusion of the dopants must be minimized. This also helps in minimizing process-induced crystallographic damage, wafer warpage and contamination by diffusion of impurities.

1.1.2.1 Overview of Chemical Vapor Deposition Process: The individual process steps in the CVD technique are outlined as follows[42]:

1. Mass transport in the bulk gas flow region from the reactor inlet to the deposition zone.
2. Gas phase reactions leading to the formation of film precursors and byproducts.
3. Mass transport of film precursors to the growth surface.
4. Adsorption of film precursors on the growth surface.
5. Surface diffusion of film precursors to growth sites.
6. Incorporation of film constituents into the growing film.
7. Desorption of byproducts of the surface reactions.
8. Mass transport of byproducts in the bulk gas flow region away from the deposition zone towards the reactor exit.

Schematically, this is seen in Figure 1.1.

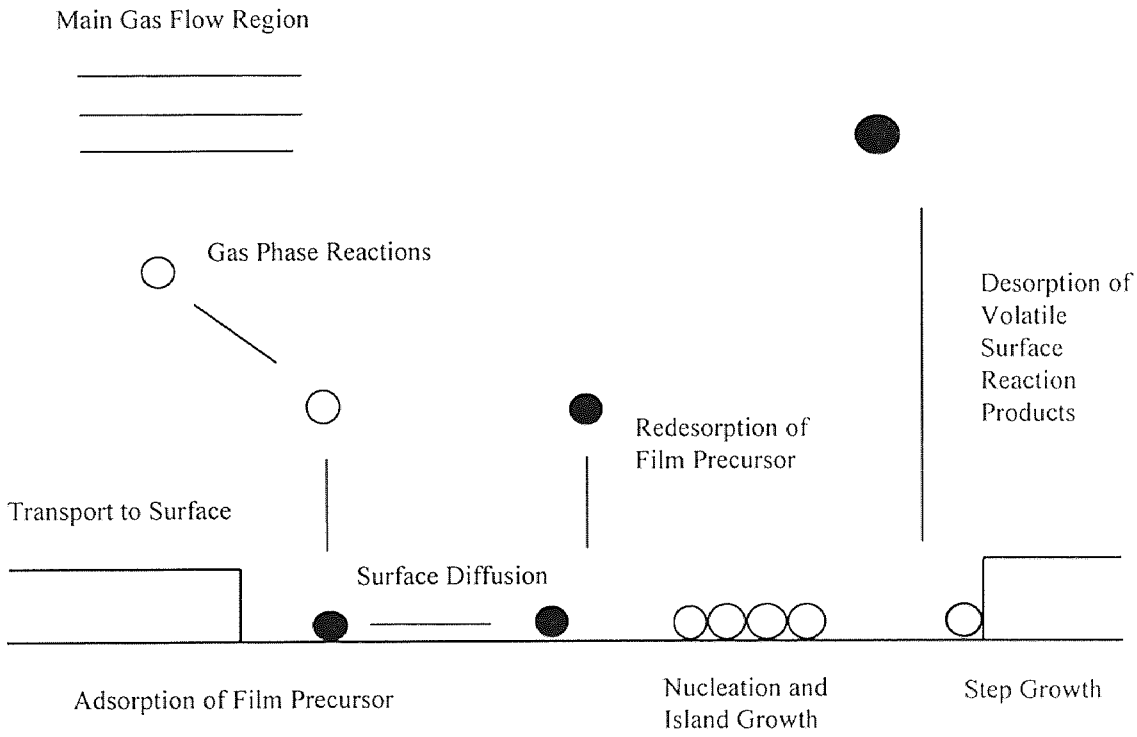

Figure 1.1: Scheme to show the transport and reaction processes underlying CVD.

1.1.2.2 CVD Reactor Systems: CVD reactors are designed to obtain optimal film thickness, crystal structure, surface morphology, and interface composition. A CVD reactor system typically consists of a reagent handling arrangement for delivering the source compounds, a reactor unit, and an exhaust system. The reagent handling system mixes and meters the gas mixture to be used in the reactor. The design depends on the source compounds. Gaseous sources are fed from a high-pressure gas cylinder through a mass flow controller, in this case nitrous oxide. Liquid and solid sources are typically used by contacting them with a carrier gas in a bubbler. The source temperature, carrier

gas flow rate, and the total pressure of the source determine the amount of reagent transported from the bubbler. In this study, a carrier gas is not needed because of the high vapor pressure of DES and the low pressure nature of the deposition. The need for films with reproducible and controllable optical, electrical, and mechanical properties means that CVD reagents must be pure, must not produce byproducts that incorporate into the growing film or interact with gas handling and reactor construction materials.

There are a wide variety of CVD reactor geometries used to accommodate the many CVD applications. These include horizontal reactor, vertical reactor, barrel reactor, pancake reactor, and multiple-wafer-in-tube LPCVD reactor. Essentially, this study involves a multiple-wafer-in-tube LPCVD (low pressure chemical vapor deposition) reactor . LPCVD is the main production tool for polycrystalline silicon films, especially for the films used in the microelectronics industry[43-45]. A typical configuration for this reactor is shown in Figure 3.1. This reactor operates around 0.05 torr and wall temperatures are approximately equal to those of the deposition surfaces. The main advantage of LPCVD is that is allows a large number of substrates to be coated simultaneously while maintaining film uniformity. This is a result of the large diffusion coefficient at low pressures, which makes the growth rate limited by the rate of surface reactions rather than the rate of mass transfer to the substrate.

Finally, the exhaust system treats the effluents so that hazardous byproducts are disposed of in a safe and environmentally sound manner. Mechanical pumps are typically added for the low-pressure operation. Dry and wet chemical scrubbers, as well as pyrolysis units, are used to clean up the reactor effluent.

1.1.2.3 Nucleation and Growth: The growth of a thin film by CVD is initiated by exposing a substrate to the film precursors in the reactor. The resulting growth and microstructure of the film is determined by surface diffusion and nucleation processes on the growth interface, which are influenced by the substrate temperature, reactor pressure, and gas-phase composition. An amorphous film is formed at low temperatures and high growth rates when the surface diffusion is slow relative to the arrival of film precursors. At high temperatures and low growth rates, the surface diffusion is fast relative to the incoming flux, allowing the adsorbed species to diffuse to step growth and to form epitaxial layers replicating the substrate lattice. Nucleation occurs at many different points on the surface at intermediate temperatures and growth rates. Adsorbed species then diffuse to the islands that grow and coalesce to form a polycrystalline film. The presence of impurities increases the nucleation density. CVD film growth modes may be characterized in terms of three main growth models for thin films: Volmer-Weber growth (three-dimensional island growth), Franck-van der Merwe growth (two-dimensional layer by layer), and Stranski-Krastanov growth (layer plus island)[42].

1.1.2.4 Chemical Reactions and Kinetics: The versatility of the CVD technique is demonstrated through the multitude of films synthesized by various reaction schemes, including pyrolysis, reduction, oxidation, and disproportionation of the reactants. The underlying chemistry is typically a complex mixture of gas-phase and surface reactions. The fundamental reaction pathways and kinetics have been investigated for only a few well characterized, industrially important systems.

1.1.2.5 Transport Phenomena: Fluid flow, heat transfer, and mass transfer are all characterized under transport phenomena. Transport phenomena govern the access of film precursors to the substrate and influence the degree of desirable and unwanted gas-phase reactions taking place before deposition. The complex reactor geometries and large thermal gradients of CVD reactors lead to a wide variety of flow structures impacting film thickness and composition uniformity, as well as impurity levels. Direct observation of flow is difficult because of a lack of a suitable visualization technique for many systems and because of practical constraints such as no optical access and possible contamination of a production reactor. Therefore, experimental observations and approximately chosen computer models are employed on individual systems[45].

The sequential steps of deposition process can be grouped into (i) mass transport-limited regime and (ii) surface-reaction-limited regime. If the mass transfer limits the deposition process, the transport process occurred by the gas-phase diffusion is proportional to the diffusivity of the gas and the concentration gradient. The mass transport process that limits the growth rate is only weakly dependent on temperature. On the other hand, it is very important that the same concentration of reactants be present in the bulk gas regions adjacent to all locations of a wafer, as the arrival rate is directly proportional to the concentration in the bulk gas. Thus, to ensure films of uniform thickness, reactors that are operated in the mass-transport-limited regime must be designed so that all locations of wafer surfaces and all wafers in a run are supplied with an equal flux of reactant species.

If the deposition process is limited by the surface reaction, the growth rate, R, of the film deposited can be expressed as $R = R_o * \exp(-E_a/RT)$, where R_o is the frequency

factor, E_a is the activation energy - usually 25-100 kcal/mole for surface process, R is the gas constant, and T, the absolute temperature. In the operating regime, the deposition rate is a strong function of the temperature and an excellent temperature control is required to achieve the film thickness uniformity that is necessary for controllable integrated circuit fabrication.

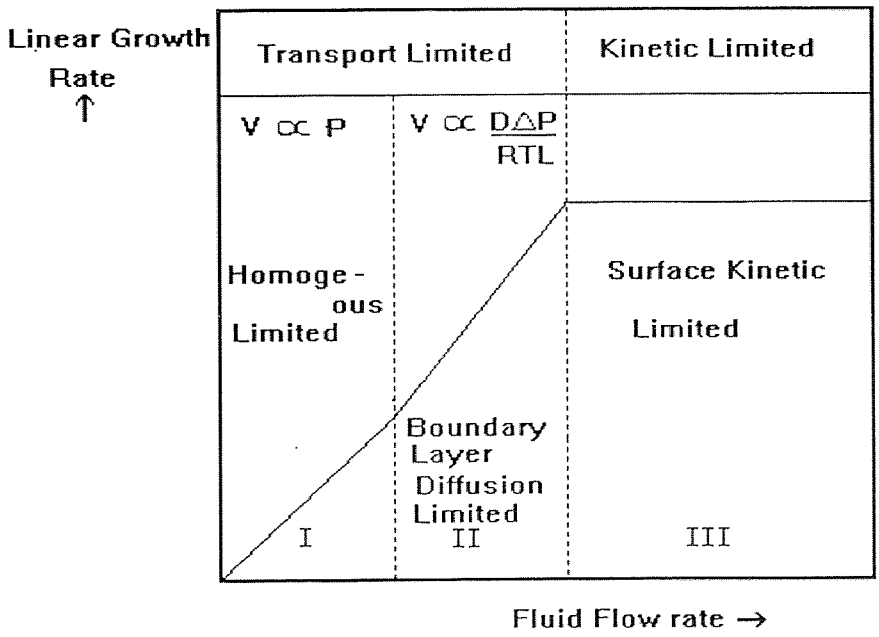

Figure 1.2 Deposition rate as a function of reactant flow rate

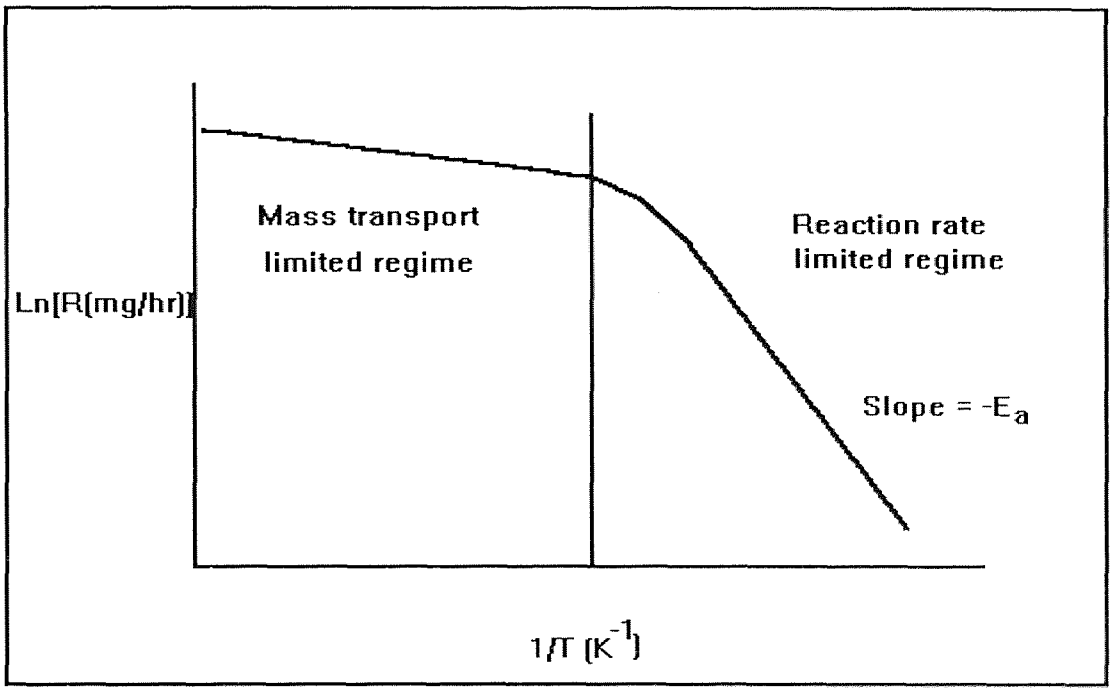

Figure 1.3 Deposition rate as a function of substrate temperature exemplifying diffusion controlled and surface-reaction controlled regimes

On the other hand, under such conditions the rate at which reactant species arrive at the surface is not as important. Thus, it is not as critical that the reactor be designed to supply an equal flux of reactants to all locations of the wafer surface. It will be seen that in horizontal low-pressure CVD reactors, wafers can be stacked vertically and at very close spacing because such systems operate in a surface-reaction-rate limited regime. In deposition processes that are mass-transport limited, however, the temperature control is not nearly as critical. As shown in Figure 1.3, a relatively steep temperature range, and a milder dependence in the upper range, indicating that the nature of the rate-controlling step changes with temperature.

1.1.2.6 Factors Affecting Film Uniformity: Some of the main factors affecting the film thickness uniformity in LPCVD are the temperature profile in the reactor, the pressure level in the reactor and the reactant gas flow rates. To obtain a flat thickness profile across each substrate wafer throughout the reactor requires a judicious adjustment of these parameters. In tubular reactors, increase in temperature or pressure, increases the deposition rate upstream, thereby using up more reactant gases and leaving less to react at the downstream end; the opposite effect takes place on lowering the temperature and pressure. Similar effects occur with variations of the reactant gas flow rates at constant gas partial pressure, or with changes in the size and number of the wafers processed per deposition run. The uniformity of thickness and step coverage of these films are very good. These films have fewer defects, such as particulate contaminants and pinholes, because of their inherently cleaner hot wall operations and the vertical wafer positioning that minimize the formation and codeposition of homogeneously gas phase nucleated particulates.

1.1.2.7 Advantages of CVD: Thin films are used in a host of applications in VLSI fabrication, and can be synthesized by a variety of techniques. Regardless of the method by which they are formed, however, the process must be economical, and the resultant films must exhibit uniform thickness, high purity and density, controllable composition and stoichiometries, high degree of structural perfection, excellent adhesion and good step coverage. CVD processes are often selected over competing deposition techniques because they offer many advantages.

The following are the advantages of CVD processes:

1. A variety of stoichiometric and non-stoichiometric compositions can be deposited by accurate control of process parameters.
2. High purity films can be deposited that are free from radiation damage without further processing.
3. Results are reproducible.
4. Uniform thickness can be achieved by low pressures.
5. Conformal step coverage can be obtained.
6. Selective deposition can be obtained with proper design of the reactor.
7. The process is very economical because of its high throughput and low maintenance costs.

1.1.2.8 Limitations of CVD: Fundamental limitations of CVD are the chemical reaction feasibility and the reaction kinetics that govern the CVD processes. Technological limitations of CVD include the unwanted and possibly deleterious but necessary by-products of reaction that must be eliminated, and the ever present particle generation induced by homogeneous gas phase nucleation that must be minimized.

1.2 Wide Bandgap Semiconductors

There is an increasing interest in semiconductors with bandgaps above 2.0 eV, since these materials offer remarkable optoelectronic devices. At present the technology for such materials is rather underdeveloped and serious hurdles need to be overcome. Some of the motivations for large bandgap semiconductor devices are discussed.

Motivations for large bandgap semiconductor:

1. **High temperature operation:** High temperature operation of electronic devices is limited by several constraints. An important constraint is the intrinsic carrier concentration of the material. Once the intrinsic concentration, determined by the bandgap and temperature, starts to become comparable to the dopant concentration, the control of the device becomes difficult. Also at high temperatures, there could be problems related to the dopant diffusion, contact stability, and, of course, ultimately defect generation and device breakdown. The high bandgap materials not only have low intrinsic concentration at a given temperature, but are also physically harder and more robust.
2. **Radiation Hardness:** An important source of error in computational devices is radiation induced errors. These errrors are generated by bursts of charges produced by cosmic rays impinging on the devices, and becomes especially important for space applications. The change burst produced by the cosmic ray (γ-rays) depends upon the bandgap of the semiconductors and can be reduced substantially by increasing the semiconductors bandgap.
3. **High Power Devices:** High power devices are extremely important for microwave applications. The power output depends upon the voltage swing across the device and the breakdown voltage of the device limits this. The breakdown voltage increases with material bandgap and thus one expects these materials to provide high power devices.

4. **Short Wavelength Lasers:** Optical memories such as compact discs are limited in their density by the wavelength of the laser diode used to read the information. Currently this wavelength is ~ 0.8 μm and the technology is based on red light GaAs lasers. There is a tremendous motivation to use blue or even shorter wavelength light to increase the memory density.
5. **Special Purpose Applications:** A number of special purpose applications can be fulfilled if a wider selection of device response is available. The motivation may come from special windows in atmospheric absorption at earth or in outer space.

While there is a clear need for large bandgap semiconductor technology, there are many hurdles as well. Some of the difficulties are:

- Crystal Growth
- Alternate Substrate Problems
- Intrinsic Defect Density
- Extrinsic Doping
- Processing of Devices

1.2.1 Boron Nitride as a Wide Bandgap Semiconductor

The wide bandgap nitride semiconductors have been of great interest for some time. It is interesting to note that the materials could occur in either the zinc blende or wurtzite form. An important problem associated with the crystal growth of nitrides is that there is a high degree of nitrogen vacancies, which appear to act as n type impurities.

Nevertheless, increased interest in high power devices is expected to allow the technological problems to be solved.

1.3 Dielectric Materials

A dielectric is a material of low dc electrical conductivity and hence a good insulator or storage medium of electric energy as in a capacitor. Their major functions have been for the isolating circuit elements, impurities, masking against oxygen and dopant diffusion, passivating and protecting device surfaces, insulating double-level conductor lines, and tapering or planarizing the device topography.

The requirements of these dielectric materials in the form of thin films for VLSI circuits for high density devices featuring linewidths in the low micron to submicron range, should have minimal structural defects and good step coverage. The particle density must be as low as possible, and the size of the particulate contaminants should not exceed 25% of the smallest feature size in the integrated circuit to avoid electrical failures or device reliability problems.

1.3.1 Requirements of Dielectric Materials for VLSI Technology

Dielectric films for insulating applications of multiple level VLSI devices must sustain relatively high dielectric breakdown fields, should have a low dielectric constant (to minimize the parasitic capacitance between conductors) and a high electrical resistivity, must have a low loss factor for high frequency applications, must be free of pinholes and microcracks and should have a low compressive stress and excellent adhesion properties. In addition, depending on the layer structure, some of the films must allow hydrogen to

diffuse through to allow removal of interface states by annealing in hydrogen, and be able to block alkali ions. All films must be readily depositable at temperatures compatible with the device structural materials and device performance requirements, with excellent compositional control and good step coverage. There materials must be patternable by precision lithography and selective etching.

Table 1.2 Desired dielectric constant (K) for future technologies [4]

Technology (MFS* in μm)	Maximum number of wiring levels**	Dielectric	K	Year
0.35	4 – 5	SiO_2 or SiO_2 (F)	3.9	1995
0.25	5	Polymer	3 – 3.7	1998
0.18	5 – 6	Polymer	< 3	2001
0.13	6	Polymer	≤ 2 – 5	2004
0.1	6 – 7	Polymer / aerogels / air	1 – 2	2007
0.07	7 – 8	Polymer / aerogels / air	1 – 2	2010

* MFS = minimum feature size; ** microprocessor

1.3.2 Requirements for low Dielectric Constant ILD Materials

The requirements for interlayer dielectric materials is summarized in the following table.

Table 1.3 Properties of ILD [4]

Electrical	**Mechanical**	**Chemical**	**Thermal**
K, anisotropy	Film thickness/ unif	High chemical resist	High th. stability
Low dissipation	Adhesion	High etch sel	T_g
Low leakage	Low stress	Low moist abs	Low TCE
Low charge trap	High tensl modulus	Low sol in H2O	Low th. shrink

1.3.3 Applications of Dielectric Materials in VLSI Technology

A. In device structures for

- isolation of circuit elements
- vertical insulation of high-temperature conductor levels in multilevel structures (polysilicon, silicides, refractory metals)
- vertical insulation of low-temperature conductor levels in multilevel structures (aluminum and its alloys)
- alkali ion and moisture barrier
- impurity gettering
- contour leveling or planarization
- over-metal top passivation

B. For temporary layers and processing aids as

- masking structures against oxidation
- gettering layers for impurities
- sacrificial material in lift-off patterning

1.3.4 BN as a Dielectric Material

CVD BN has unique properties because it is usually highly oriented, which emphasizes the effect of the layered structure. The boron and nitrogen atoms are 1.46 Å apart in the ab plane and the layers are separated by 3.34 Å. Thus properties such as thermal expansion and electrical resistivity differ in directions parallel and perpendicular to the substrate surface.

Some of the attractive properties of BN are its low deposition temperature, high insulation, high passivation effects against moisture and the alkali metal ions, conformal step coverage, high crack resistance and chemical inertness. It starts dissociating at 2700°C in vacuum and is oxidized in air only at temperatures as high as 1200°C. It has a reported dielectric constant close to that of silicon dioxide and electrical resistivity in the order of 10^{14}ohm-cm with a dielectric strength in the order of 10^6 V/cm and an optical band gap of 4-6 eV. This makes a good material to study the electrical properties.

Table 1.4 Properties of CVD boron nitride dielectric [11]

Tensile strength (ksi)	6
Modulus (Msi)	3.6
Flex strength (ksi)	15
Poisson's ratio	-0.025
Thermal conductivity (W/M.K)	a-62.7 c-1.45
Coeff. T.E. (10^{-6})	a-3.24 c-81
Electr. Resist. (ohm-cm, 437 /°C)	a-3 x 10^7 c-3 x 10^9
Dielectric strength (V/mil)	c-4000
Dielectric constant (5 x 10^9 Hz)	a-5.1 c-3.4
Loss tangent	3 x 10^{-4}
Density (g/cm^3)	2.22
Melting point	3000 °C

1.4 Triethylamine Borane Complex as a Precursor

Extensive work has been done on the chemical vapor deposition of BN thin films on various substrates including silicon, quartz, and glass. A wide range of precursors have been used to obtain these thin films which include diborane, borontrichloride, triethyl boron, dicarborane and borane triethylamine (TEAB) complex. TEAB has several advantages over many of the other precursors. Table 1.5 gives some of the properties of TEAB.

TEAB is a relatively non-toxic and non-pyrophoric substance and this obviates the need for expensive cabinets and a cross-purging gas supply for safety reasons. However, TEAB has a low vapor pressure and hence has to be forced into the reactor under high pressure.

Table 1.5 Properties of TEAB

Chemical name	Borane triethylamine complex (TEAB)
Chemical formula	$(C_2H_5)_3N.BH_3$
Molecular weight (g/mol)	115.03
Specific gravity (g/cc)	0.777
Freezing Point	-3°C
Boiling point	97°C
Appearance	Colorless liquid
Vapor pressure	20 Torr at 97°C
CAS Registry number	1722-26-5

CHAPTER 2

REVIEW OF LITERATURE OF BN FILMS

2.1 Introduction

In this chapter a review of the deposition techniques of boron nitride thin films and their properties will be discussed. A brief review of the electrical characteristics, including the current-voltage, electrical resistivity and the dielectric constant of thin films in general and BN and SiBN films in particular will be discussed. Finally, the aim and scope of this work will be discussed.

2.2 Deposition Techniques

Thin films of boron nitride have been grown on various substrates including copper, steels, silicon, quartz, sapphire and fibers. The techniques used (Table 2.1) have included chemical vapor deposition (CVD) [1-17], low pressure chemical vapor deposition (LPCVD) [18,19], plasma assisted CVD [14,20-24], reactive sputtering [25,26], electron beam irradiation [27], ion beam deposition [28-30],ion plating and pulse plasma method [31-33]. Boron sources have included diborane [1-4,14,18,20], boron trichloride [12-16,22], borazene [19], triethyl amine borane complex [23,24] dicaborane [17], hexachloroborazene [6], Organoamine boranes [6], B-vinylborazenes [6], 2-vinyl-pentaborane [6] and 2,4,6-B-triamino-1,3,5-N-triphenylborazene [6].

In this section a review of the synthesis of boron nitride by chemical vapor deposition and LPCVD techniques is done, as it is relevant to the present work.

Table 2.1 Synthesizing techniques of boron nitride thin films

Technique	Reactants	Remarks	References
CVD	B_2H_6, NH_3, H_2, N_2	Deposition temp. 400-1250°C, max. Deposition rate at 800°C, clear, vitreous films	1, 4, 9
CVD	BCl_3, NH_3, H_2 (Ar)	Deposition temp. 250°-1250°C, films deposited below 450°C are unstable in moist atmosphere, transparent and smooth films are produced between 1000° and 1200°C	12 - 16
MFCVD	$B_{10}H_{14}$, NH_3	Stoichiometric films are deposited at temp. Of about 850°C	17
LPCVD	B_2H_6, NH_3	Physical and optical properties of the films formed at temp. 300°-400°C are stable and inert towards water and aqueous solutions	18, 20
LPCVD	Borazine	Films formed at temp. 300°-400°C react with atmospheric moisture	19
PECVD	B_2H_6, NH_3	Deposition temp. 1000°C, polycrystalline structure appears	14
PECVD	B_2H_6, NH_3	Deposition temp. 550°-620°C, amorphous structure	22
PECVD	$BH_3N(C_2H_5)_3$, NH_3	Deposition temp. 200°-350°C, amorphous structure, good electrical properties	23 - 24
Sputtering	B, BN, N_2 (Ar)	Films can be deposited without heating the substrate	25, 26
Electron beam evaporation	BN	Stable amorphous structure, deposition temp. 1050°C	27
Ion beam deposition	B, N_2, NH_3 (Ar)	Ion beam plating of e-beam evaporated boron	28 - 30
Ion beam deposition	$B_3N_3H_6$ (Ar)	Plasma decomposition	28 - 30
Pulse plasma method	B_2H_6, B, N_2, H_2	Plasma decomposition, cubic structure	31 - 33

2.2.1 Synthesis by CVD Technique

CVD BN can be prepared from BCl_3 and NH_3, BF_3 and NH_3, B_2H_6 and NH_3, borazine, trichloroborazine, borontriethylamine and NH_3. Four reactions for forming CVD BN are most common. They are:

$$BCl_3 + NH_3 = BN + 3HCl$$

$$B_3N_3H_3Cl_3 = 3BN + 3HCl$$

$$B_3N_3H_6 = 3BN + 3HCl$$

$$BF_3 + NH_3 = BN + 3HF$$

The reaction involving BCl_3 forms an amorphous material at temperatures of 1100°C and below [11] and dense hexagonal BN in the temperature range of 1600 to 1900°C with pressures below 2 torr.[11]. The orientation improved with increasing deposition temperatures, but crystallinity can also be attained at lower temperatures by the use of plasmas[11]. Better crystallinity can also be obtained by using low pressures.

When hydrogen was included with BCl_3 and NH_3, it resulted in less crystallinity, decreased moisture resistance, and free boron and chlorine incorporation in the deposits. Oxygen and carbon inclusions tend to break up the hexagonal deposits. Baronian [11] used this BCl_3-NH_3 system to form CVD BN films at deposition temperatures from 600 to 900°C on a quartz substrate heated by inductive coupling to a graphite susceptor. The gas flows were 230 cc/min of NH_3 and 25 cc/min of BCl_3, and the gas pressure was held between 200 and 600 μm to obtain a deposition rate of 50 Å/min. the refractive index of these films ranged from 1.9 to 2.0.

The BCl_3-NH_4 system was also studied by Matsuda et al. [11] but with H_2 addition, over a temperature range of 1200 to 2000°C and a pressure of 5 to 60 torr. The BCl_3 and the dilution gas H_2 were introduced in an outer tube and NH_3 in the inner tube at a rate of 90, 670, and 140 cm3/min, respectively, and passed over a hot graphite substrate. The gases were kept separate so as to prevent white powder formation.

The flow rates used were 0.1 ml/s of BCl_3, 0.5 ml/s of NH_3, 0.4 ml/s of H_2 and 0.7 ml/s of argon at 1200°C to produce a hexagonal material. An amorphous phase was white, while the crystalline phase was translucent. The crystalline phase was stable in air from 20 to 900°C.

Takahashi et al. [11] also studied the BCl_3-NH_3 system for preparing CVD BN, but they also used H_2 and an argon diluent and carbon steel as a substrate. Care was taken in their process to add the BCl_3 and Ar and NH_3 + H_2 in two separate tubes to 2 cm above the substrate to prevent NH_4Cl from forming on the wall of the reactor.

Kuntz [11] formed CVD BN using BF3 and NH3 using temperatures from 1600 – 1700 °C and pressures below 2 torr. The material produced was highly crystalline. The BF3 reaction tends to be much cleaner. Hexagonal deposits have been prepared at lower temperatures and BF3 is less apt to produce boron in the deposit. Pierson [11] produced these hexagonal BN deposits at only 1100°C and pressures of 30 – 40 torr.

Many investigators [1-4] have deposited BN thin films from diborane and NH_3 using an inert carrier gas according to the reaction

$$B_2H_6 + 2NH_3 = 2BN + 6H_2$$

Rand et al. [1] used many substrates such as Si, Ta, Mo, Ge and fused silica, at various temperatures ranging from 600°C to 1080°C. The typical deposition rates varied from 12.5 to 60 nm/min. in H_2 or He and 100 nm/min. in nitrogen. The dependence of the deposition rate on temperature and NH_3 to B_2H_6 ratio was found to be complex. The deposition rate exhibited a maximum at 800°C and it decreased as the NH_3/B_2H_6 ratio was increased from 10:1 to 20:1.

Makoto Hirayama et al [10] deposited amorphous and polycrystalline boron nitride films on n-type Si substrates using a B2H6-NH3-H2 system. When the deposition temperature was below about 1000°C, the film was amorphous. When the deposition temperature was over 1000°C, the film was polycrystalline with a hexagonal structure. During deposition of BN films, boron diffused into the silicon substrates. BN films thicker than 500 Å deposited below 1000°C acts as infinite diffusion source of boron. When these films were used as diffusion source, the maximum values of boron surface

concentration correspond to the solid solubility of boron in Si at each temperature. A thin BN film (about 80Å deposited at 700°C) gave a surface concentration of boron in the range between 10^{16} and 10^{20} cm^{-3} by varying the prediffusion heat-treatment conditions.

Murarka et al. [9] studied the growth process on silicon substrates. The deposition rate was proportional to the flow rate of B_2H_6 and to the negative fifth power of the flow rate of NH_3. For a fixed NH_3/B_2H_6 ratio, the deposition rate increased linearly with the flow rate. The deposition rate increased with temperature in the temperature range 400°C to 700°C, and at higher temperatures, the reaction was nearly independent of temperature. Hirayama et al. [10] also used Si substrate, maintaining the substrate temperatures ranging from 700°-1250°C. The growth rate of the film was about 50nm/min. at 700°C.

Baronian [12], Motojima et al. [14] and Takahashi et al. [15,16] used BCl_3 and NH_3 with the following reaction

$$BCl_3 + NH_3 = BN + 3HCl$$

Baronian [12] deposited BN thin films on quartz substrates at temperatures ranging from 600°-900°C. Motojima et al. [14] used Cu substrates at temperatures in the range 250°-700°C. The films deposited at temperatures below 450°C were unstable in a moist atmosphere.

Takahashi et al. [15,16] studied in detail the effect of the substrate material on the growth process. According to their results, Fe and Ni were the favorite elements for forming BN crystalline deposits. The formation of the first layer of BN was initiated by a catalytic action of the Fe atoms.

Nakamura [17] proposed a new CVD method in the molecular flow region (MFCVD) for depositing BN films using $B_{10}H_{24}$ and NH_3 reaction gases at substrate temperatures between 300° and 1200°C. He has reported that the decomposition of the films could be closely controlled by regulating the pressure of the source gases and stoichiometric BN films could be deposited at $NH_3/B_{10}H_{24}$ ratios of 20 or more at a substrate temperature.

2.2.2 Synthesis by LPCVD Technique

A.C. Adams and C.D. Capio [20] deposited films of a boron-nitrogen compound with a composition of approximately B_6NH_x at reduced pressure by reacting diborane and ammonia at 250° - 600°C in an LPCVD reactor. The thickness uniformity was within ± 3% for films deposited at 350°C. Infrared spectra showed that the films contain boron and nitrogen, possibly bonded in a ring structure and hydrogen bonded as BH, NH_2, and possibly NH. The film properties are nearly independent of the ratio of the reactants, but are affected by the deposition temperature. The film refractive index is about 2.2 for films deposited at 340°C. At 600nm, the absorption coefficient is about 2.5 x 10^4 cm^{-1} and increases with increasing temperature. The films were chemically inert, being insoluble in all the etching solutions investigated. However the films are easily etched in a CF_4-O_2 plasma. The step coverage is conformal with no pin holes and surface defects.

Levy et al [5] studied the microstructure of amorphous hydrogenated LPCVD boron nitride films with respect to hydrogen bonding and distribution. NMR, ESR and EGA techniques were used in the characterization. It was found that the hydrogen is

essentially randomly distributed as monohydrides; other configurations such as dihydrides and monohydride clusters, are estimated to be less than 20% total.

2.3 Properties of Boron Nitride Films

In this section the mechanical, optical, chemical, thermal and radiation hardness are discussed. It is found that the structure of the BN thin films are amorphous or polycrystalline (hexagonal or cubic) depending on the method of synthesis. Table 2.2 gives a few details of the properties of BN films based on the method of synthesis. The density [20] of the BN films is 1.7-2.1 gm/cc.

Table 2.2 Properties of BN thin films

Deposition technique	Refractive index	Optical band gap (eV)	Dielectric constant	Electrical resistivity (Ω-cm)	Dielectric strength (V/cm)	References
CVD	1.7 - 1.8	3.8	3.7	10^{14}	5×10^{6}	1
CVD	1.7 - 2.8	-	-	-	-	9
CVD	-	-	3.3 - 3.7	10^{9} - 10^{10}	10^{7}	4
CVD	1.9 - 2.0	5.83	-	-	-	12
CVD	-	5.8 - 6.2	-	-	-	13
CVD	-	-	-	-	-	14
CVD	1.65	-	-	10^{14}	-	15
MFCVD	-	5.9	-	-	-	17
PECVD	-	-	2.7 - 7.7	10^{9}	-	21
PECVD	-	-	3.5	-	7×10^{6}	23,24
PECVD	1.746	4.7	3.8 – 5.7	-	7×10^{6}	34
Sputtering	-	4.9 - 5.6	3.8	-	-	25
Sputtering	1.6 - 1.9	3.3 - 5.6	-	-	-	26
Ion beam dep.	-	-	-	10^{10} - 10^{14}	-	30
Plasma pulse method	1.5 - 1.6	5.0	5.6 7.0	10^{16}	10^{6}	33

The chemical composition of the films depends on several experimental parameters. Films synthesized by r.f. sputtering [26] in argon gas discharge have an excess of boron and BN. However, by controlling the experimental parameters, stoichiometric BN thin films can be grown. It was also found that boron nitride thin films prepared by ion beam deposition method [28,29] contain a considerable amount of oxygen and those obtained from pulse plasma method [33] show the presence of microinclusions of B_2O_3 and boron. Some films react with moist atmosphere. The intrinsic cause of such a reaction was reported [1,23] to be due to the presence of oxygen at the time of deposition.

The IR spectrum of a film deposited on silicon shows two typical absorption bands. A strong asymmetrical band at 1400 cm^{-1} is attributed to B-N bond stretching. A weaker sharper band at 800 cm^{-1} is attributed to B-N-B bond bending. The broadness and frequency shifting of the BN stretching vibration band depend on experimental conditions. The adherence of the films depends on the substrate material and deposition conditions. However, the adherence of the films has been generally satisfactory. The films deposited at reduced pressure at 340°C have a lower stress at all NH_3 to B_2H_6 ratio is less than about 0.3; at higher ratios, the film stress is compressive. For the B-H-N structure [20], the hydrogen content affects the stress. When the hydrogen content is less than about 21 atom percent, the films are under tensile stress and, for hydrogen concentrations of about 24 atom percent, the films are under compressive stress.

The thermal stability of the BN films depends on the deposition conditions. For example, the films deposited by CVD [14] at above 600°C were stable decreased in mass by 1-2 percent on heating and were stable in air at temperatures below 750°C. For films

deposited at temperatures over about 1000°C, no changes were observed in the polycrystalline patterns even after a long treatment [4] in hydrogen or nitrogen for several tens of hours at 1250°C. However, amorphous films deposited below 1000°C were decomposed during heat treatment in nitrogen [4].

The boron nitride films are chemically stable and cannot be attacked by etching solutions except for phosphoric acid [1,4,20]. The etch rate of the film [4] is about 8 nm/min. in a solution of equal volumes [1] of deionized water and phosphoric acid at 130°C and 15 nm/min. in phosphoric acid at 180°C. The films can be etched easily in a CF_4-O_2 [20] plasma, but the etch rate depend on the deposition temperature of the film. The optical band gap and the refractive index vary according to the experimental parameters and boron-to-nitrogen ratio. The reported values of the band gap lie in the range from 3.3 to 6.2 eV (Table 2.2) and the refractive index from 1.5 to 2.8. In the visible region, the stoichiometric BN film is highly transparent and colorless but, on increase in the boron-to-nitrogen ratio in the film structure, the color becomes pale yellow, deep brown or light golden [26].

BN films are good electrical insulators. Their electrical resistivity is about 10 Ω-cm at room temperature and 10^3 at 200°C. The dielectric constant is about 4. BN films have a low dielectric loss at frequencies ranging from dc to microwave. The dielectric breakdown field strength is about 10V/cm.

The chemical composition of the films prepared by LPCVD [18-20] differs from stoichiometric BN film and these films are called *borohydronitride* (B-H-N) films. Johnson et al. [35] reported that B_3NH films produced using LPCVD in a manner similar

top that used by Adams and Capio [20] were susceptible to radiation damage from 1-3 KeV X-ray radiation. This would lead to pattern distortion and shorten the life span of the masks. They related the problem to hydrogen content of the film and there by the deposition temperature of the film. Levy et al. [36] showed that the heat treatment of the film resulted in the loss of the hydrogen bond to the ammonia at around 700°C and the loss of hydrogen bond to the boron at around 1100°C. The result indicated that the conduction follows the Frenkel-Poole emission mechanism. The current-voltage (I-V) characteristics of BN films are non linear. The conduction mechanism through BN films is either Schottky type (Poole-Frenkel) or space charge limited depending upon the conditions of the film deposition.

2.4 Applications

CVD BN has been well known as a release agent and has been used in crucibles because, it is chemically inert to many reagents and metals in a temperature range of 1020 to 2020°C. It doesn't react with graphite at 2220°C and reacts only slightly with W at 2020°C. It has been immersed in boiling water for extended periods without any changes.

It can also be used as an electrical insulator or heat shield especially when it is highly oriented so the basal planes are perpendicular to the electrical current or heat flow. Because of its high dielectric strength, it can also be used in high temperature capacitors. BN films can be used as an insulator in a metal-insulator-semiconductor (MIS) memory diode[4].

BN films form a transparent substrate for X-ray lithography mask [20,37,38]. The BN mask is inexpensive and easy to fabricate, highly transparent to Pd L X-rays and

dimensionally stable through all phases of mask processing. This mask is also optically transparent to facilitate reregistration.

BN films are useful as a restricted-area boron diffusion source. This method can be used to fabricate planar diodes using only one photomask. The n type Si wafers are thermally oxidized to about 300 nm, and the windows are opened in the silicon dioxide. Next a BN film is deposited. To diffuse the boron in the windows, the BN film must be decomposed. For this, the samples are heated in nitrogen atmosphere at 1100°C for about 120 minutes. Boron diffuses into the silicon through the windows, and the bare silicon surface appears on the windows. Then, to make ohmic contacts, Ni can be deposited directly by electroless plating on bare silicon surfaces of the windows and on the back face of the silicon wafer. Thus by these processes, planar diodes can be made by using only one photomask.

BN film coatings are useful to increase the hardness of materials [28-30] as protective coatings against the oxidation of base materials.

BN thin films show a stable, strongly non-ohmic high field conductivity [1]. A film of about 100 nm thick (or thinner) may be used in integrated circuits as thin film varistors or voltage limiters.

BN films can be used as high quality insulating films [23,24] for MIS structures based on III-V compounds such as GaAs and these structures are suitable for high frequency device applications.

Other applications of CVD BN include furnace components, boats, trays and tank liners which can be used at very high temperatures in the absence of air. Even in air, the BN is protected by B2O3 until the B2O3 begins to vaporize at about 1100°C.

It can also be used as a window at 5.5μm, 12 μm and above 15 μm where it can be employed as an infrared polarizer. Its low dielectric constant of 3.4 in the c direction also makes it useful in microwave applications, such as radomes.

In addition to the above applications, CVD BN has also been used as a fiber coating in composites to densify composites and as a matrix in composites. As a fiber coating, it provides a weak bond between the fiber and matrix resulting in a tough composite. In carbon-carbon composites, it increases the oxidation resistance by protecting the carbon fibers.

2.5 Dielectric Thin Films

Within the next three years, 0.35-μm and early 0.25-μm generation devices will become available. To accommodate these smaller design rules and higher device densities, the number of interconnect levels must increase from three levels to five or possibly six. Use of more interconnect levels complicates the manufacturing process, but means that interconnect linewidths and packing densities need not shrink in proportion to the reduction in transistor gate length. This postpones the need to adopt revolutionary copper interconnect / low-k dielectric schemes. However a time will definitely come when further increase in the number of levels will not decrease the signal propagation time because the signal propagation time would be limited by the capacitance between the interconnect layers as reflected in the delay constant [39].

$$RC = \rho_m \varepsilon_{die} L^2 / d_{die}$$

Where ρ_m is the sheet resistance of the interconnect, L is the interconnect length, ε_{die} is the

dielectric constant of the interlevel dielectric (ILD), d_{die} is the thickness of the ILD, R is the resistance of the interconnect metal, and C is the capacitance of the ILD. It is evident from the relationship that a low RC constant can readily be achieved through material modification by reducing the resistance of the interconnect metal and the dielectric constant of the ILD.

A desirable ILD material should exhibit in addition to a low dielectric constant, low mechanical stress, high thermal stability and low moisture absorption. Several ILD candidates have been explored over the last few years. These have included fluorinated SiO_2 [41-51], fluorinated polyamides [52,53] and BN [54-55] films. Fluorine is the most electronegative and the least polarizable element. Therefore, incorporation of F reduces the number of polarizable geometry. These changes result in lowering polarizability of the fluorinated SiO_2 film itself, thus lowering the dielectric constant.

2.5.1 Organic Fluorinated Dielectric Films

As interconnect dimensions in integrated circuits shrink well below 0.5 μm, traditional dielectric insulators have inadequate performance. Organic polymers, in general, exhibit lower dielectric constants than inorganic oxides and nitrides, and thus are candidates for the intermetal dielectric at these small dimensions. Most organic polymers do not possess adequate thermal stability for backend processing, however. A few candidates, such as fluorinated poly(arylenethers), may prove useful if they possess sufficient dimensional stability to withstand multilayer interconnect processing.

Organic polymers, specifically polyimides, were used for integrated circuit IMD in production by IBM from the early 1970s through the late 1980s. In addition to organic polymers, many of which exhibit ε of 3 or below, at least two classes of materials are currently under investigation. One is SiO_2 that has been fluorinated by a variety of methods [46]. Another is the class of silicon-oxygen polymers called silesquioxanes, which can be thought of as high organic content spin-on glasses [46]. For subsequent generations, it appears that only a few unique and thermally stable polymers exhibit sufficiently low ε combined with other important properties and processing characteristics.

A family of thermally stable, low-dielectric constant polymers are under development at AlliedSignal Advanced Microelectronic Materials as an alternative to polyimides for IC intermetal applications. The polymers, fluorinated poly(arylenethers), are envisioned for use in devices fabricated with design rules of 0.25 μm and below. They are prepared by condensation of decafluorobiphenyl with aromatic bisphenols [46]. Compared to polyimdes, these polymers exhibit comparable thermal stability while providing significantly lower ε, lower moisture absorption, higher outgassing rates, and greater ease of processing.

Silsesquioxanes polymers typically result from hydrolysis and condensation of alkyl- or aryltrialkoxysilanes, Rsi(OR')3. With ε of 1.7 – 3.0, they may provide an intermediate dielectric solution for the 0.35 or 0.25 μm generation of devices. These materials, also under development, can contain upto 50% organic content by weight, but possess a silicon-oxygen backbone that contributes to their relatively high stability when

exposed to oxygen plasmas. The silsesquioxanes exhibit high thermal stability, low residual stress, low moisture absorption, and excellent gap filling and local planarization properties. Since they are processed in a similar fashion to spin-on glass, they may offer a much lower dielectric constant than traditional dielectrics, without the major process integration challenges that will surely accompany purely organic polymer dielectrics.

The primary means of reducing the dielectric constant and refractive index has been fluorination of the polymer backbone. This has been achieved by incorporation of hexafluoro groups and by aromatic substitution of fluorine atoms, trifluoromethyl groups, fluorinated alkoxy side chains, and more recently, pentafluoro sulfur groups. Reduction of dielectric constant in polyimides has also been achieved by introducing fluorine-containing additives and by blending Teflon into the bulk polyimide material. Control of the refractive index of polyimide waveguide materials has been achieved through copolymerization of fluorine containing monomers. It is believed that the dielectric constant and refractive index of fluorinated polyimides are reduced by a combination of mechanisms. First, the electronic polarizability is reduced through the addition of fluorine-carbon bonds. In addition, interchain charge transfer complexation and associated chain packing are impeded by bulky fluorinated side groups, by kinks in the polymer backbone, and by spacer groups. Low refractive indices in fluorinated polyimides can be accurately predicted by current property prediction techniques. This suggests that it is the fluorine atoms and the bonds in the polymer repeat unit that have the largest effect in reducing refractive index. As a result of the preferential alignment of the most polarizable groups in the polyimide, i.e., the main chain phenyl rings, control of refractive index in polyimides in and out of the plane of the film by introducing

orientation into the polymer film, increases the refractive index in the direction of orientation and reduces normal to the direction of orientation.

2.5.2 Fluorinated SiO_2 Dielectric Films

Several reports [41-51] have indicated that the dielectric constant of silicon dioxide films can be reduced with increasing amounts of F in the films. Usami et al.[41] used a parallel-plate electrode CVD system to deposit SiOF films using tetraethoxysilane (TEOS)-He-O_2-C_2F_6 gas plasma generated by r.f. power at 13.56 MHz at a temperature of 360°C and a pressure of 9 Torr. They found that the deposition rate and refractive index of the film decreases with increasing C_2F_6 flow rate. This suggested that there is a change in the film composition and also a decrease in film density with increase in C_2F_6 addition. They suggested that the Si-O bond strength was influenced by Si-F bond formation due to the high electronegativity of fluorine was the cause of reduction of refractive index due to the structural changes in the film. The dielectric constant of the SiOF films were compared before and after annealing at 400°C in a hydrogen atmosphere for 30 minutes. Before annealing, the relative dielectric constant of the conventional PE-TEOS oxide was 4.9. this value was higher than that of thermally grown silicon dioxide (3.9). This result is due to the presence of highly polarized compounds such as Si-OH and H_2O in the film. With increasing fluorine concentration, however, the relative dielectric constant decreased. It is supposed that polarization of Si-O bonds was changed with the presence of Si-F bonds due to the high electronegativity of fluorine. After annealing the relative dielectric constant was lower (4.5) than that before annealing at all fluorine concentration indicating that the highly polarized compounds such as Si-OH and H_2O content in the

films decreased even though a small amount of fluorine desorbed from the film. The least dielectric constant of 3.6 was obtained at 14 atomic % fluorine.

2.5.3 BN and SiBN Thin Films

Recent publications [54-58] have reported on the use of plasma enhanced chemical vapor deposition (PECVD) to synthesize BN and SiBN as potential low ε materials. Maeda et al. [54] deposited amorphous SiBN ternary films using a parallel plate electrode reactor using a SiH_4-B_2H_6-NH_3-Ar gas mixture at a frequency of 13.56 MHz to obtain low dielectric constant films. Strong and broad absorption bands were seen at wavenumbers 890 cm^{-1} and 1320 cm^{-1} in the IR absorption spectrum corresponding to Si-N and B-N lattice vibrations respectively. The refractive index was found to decrease with increasing B atomic ratios. An observed value of 1.71 obtained from stoichiometric boron nitride was similar to hexagonal like amorphous boron nitride films. The static dielectric constant (at 1MHz) monotonically decreased from $6.8\varepsilon_o$ of silicon nitride to $3.0\varepsilon_o$ for stoichiometric boron nitride with increasing boron atomic ratio. The optical dielectric constant also decreased with increasing boron atomic ratio to obtain a value of $2.9\varepsilon_o$ for BN. Thus the difference between the static and the optical dielectric constants was extremely small for BN films while the static dielectric constant was 1.75 times larger than the optical one for Si_3N_4. The I-V characteristics of SiBN films indicated that for silicon nitride the carrier transfer follows the hopping conduction and bulk limited Poole-Frenkel conduction in the lower and higher electrical field regions respectively.

2.6 Aim and Scope of the Present Work

The aim of the present study was

1. to synthesize boron nitride thin films
2. characterize these films
3. obtain low dielectric constant thin films.

The basis of the present work was based on the extensive research done on the synthesis and characterization of boron nitride thin films over a series of temperature from 300° to 850°C using TEAB and ammonia as the precursors.

CHAPTER 3

EXPERIMENTAL PROCEDURE

3.1 Introduction

Boron nitride thin films with varying composition were synthesized in a LPCVD reactor with a vapor phase flow system, adjusting various parameters including temperature, pressure, gas composition and time of deposition. Fourier transform infrared (FTIR) analyses were done on the synthesized films to examine the vibrational modes of the deposited films. Stress on the films was measured and calculated by the principle of radius of curvature difference. Ellipsometry and interferometry measured refractive index and thickness of the films respectively. The current-voltage (I-V), capacitance-voltage (C-V), resistivity and the dielectric constant of the films were also measured.

3.2 LPCVD Reactor

The deposition reactor is schematically shown in Figure 3.1. This reactor was manufactured by Advanced Semiconductor Materials America Inc.(ASM America, Inc.) as a poly silicon micro-pressure CVD system. The horizontal reaction chamber consists of a 13.5 cm diameter and 135 cm long fused quartz tube encapsulated with a three-zone, 10 kwatt, Thermco MB-80 heating furnace. The process tube door was constructed of a 300 series stainless steel, with a side hinge and sealed with an O-ring. At one end a heating jacket maintained the temperature of the bubbler to a constant value ranging between 0°C and 70°C, depending on the flow required. The vapors of the precursor were

passed to a vapor phase flow controller which was connected to the reactor by means of a pipe. The lines that carried the vapors of the precursor were heated to 70°C and the vapor phase controller was maintained at 90° to avoid the condensation of the TEAB. A MKS mass flow controller controls the flow of ammonia into the reaction chamber. A spare nitrogen mass flow controller was installed to incorporate any necessary additional reactant gas into the chamber or for backfilling. This spare controller could be calibrated for the gases other than nitrogen.

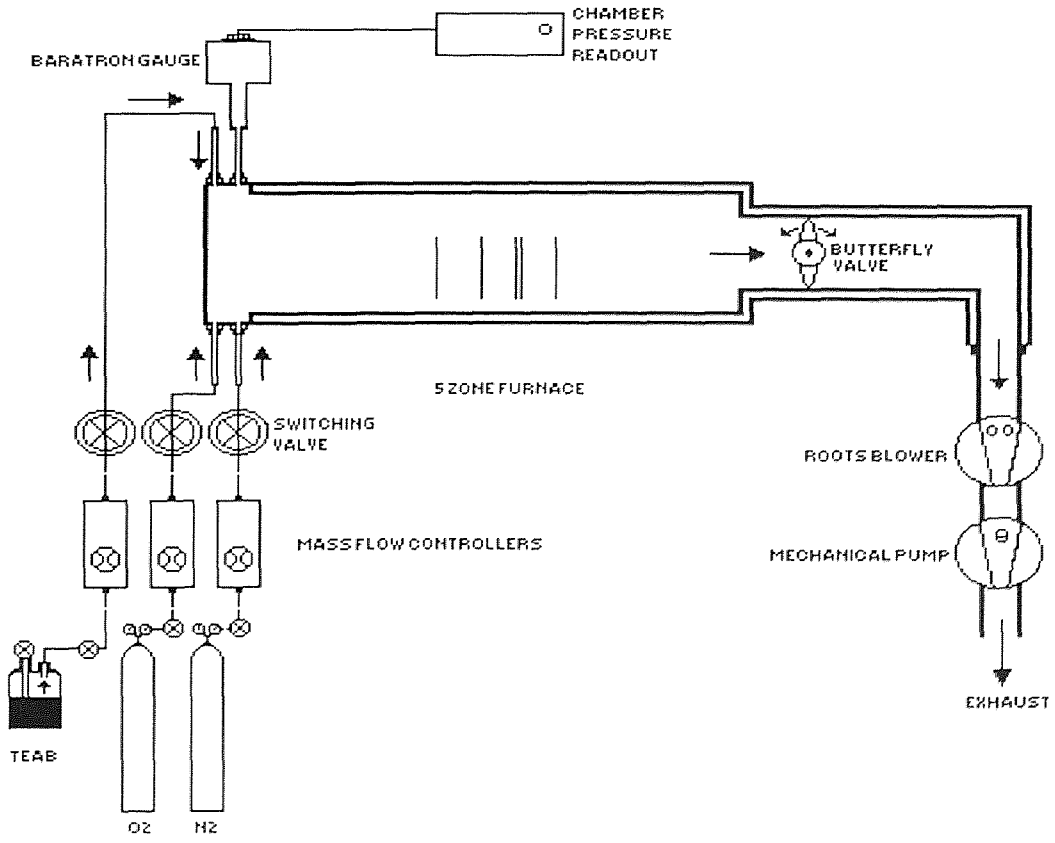

Figure 3.1 Schematic representation of the LPCVD reactor

The other end of the reaction chamber is connected to a vacuum station comprised of a Leybold-Heraeus Trivac dual stage rotary vane pump backed by a Leybold-Heraeus roots pump to create the necessary vacuum in the system. An oil filter system is used to filter unnecessary particles from oil and thereby increasing the lifetime of the pump. End caps designed for this reactor have a provision for cold water circulation to avoid overheating of the O-rings. A ceramic tube was setup between the chamber and the heater to enhance the radiation heat transfer thus reducing the temperature deviation through the reaction tube. The temperature was kept constant across all zones and confirmed using a calibrated K type thermocouple. Mass flow controller set points were programmed with a MICON 3 microprocessing controller which produces the set point voltage and automatically monitors the flow vs. the programmed flow limits. The pressure in the reactor is monitored with an automatic exhaust valve and measured at the reactor inlet using a capacitance manometer (13 Torr MKS baratron pressure gauge).

3.2.1 Vapor Phase Flow Mechanism

The vapor phase flow system, designed and fabricated in-house [42,56], consists of a stainless steel bubbler connected to a vapor phase flow controller, which is connected to the reaction chamber. The vapor phase flow system was developed on the basis of thermodynamic principles, which states that when the phases are not in equilibrium, mass transfer occurs between the phases. The rate of transfer of each species depends on the departure of the system from equilibrium. Equilibrium is a static condition in which no changes occur in the macroscopic properties of the system with time. This implies a

balance of all potentials that may cause change. If vapor and liquid are to exist in equilibrium one cannot exercise independent control over these two variables for this system. The number of independent variables that must be arbitrarily fixed to establish the intensive state of a system, i.e., the degrees of freedom F of the system, is given by the celebrated phase rule of *J. William Gibbs*, which can be given as follows:

$$F = C - P + 2$$

Where;

F = number of degrees of freedom,

C = number of components, and

P = number of phases

On applying the above equation to our system, which consists of a single component i.e., TEAB, and two phases involving the liquid and the vapor phase, we get the number of degrees of freedom to be 1. This implies that on changing one of the variables, which was temperature in our case, the pressure of TEAB in the vapor phase automatically gets fixed.

On the basis of the above principle, a heating jacket was made to cover the TEAB bubbler and by varying the temperature of the jacket, the amount of TEAB in the vapor phase was controlled. The goal was to maintain at any time sufficient vapor in the bubbler so that the vapor phase flow controller that was connected in series to the bubbler would always remain the rate-determining step in controlling the flow. The precursor used as a source of boron can slowly react with oxygen and forms an undesirable white powder contamination and hence requires handling in an inert glove box. The flow rate of the

TEAB precursor was maintained between 1 and 10 sccm for all the runs. This was achieved by maintaining the temperature of the bubbler between 40 to 65°C.

3.3 Experimental Setup

3.3.1 Leakage Check

The leak check is one of the most important steps in this experiment because the usage of a vapor phase flow system does not allow the bubbler to be maintained at a positive pressure. This results in a high probability of leakage into the bubbler. A leak would result in a change in the deposit structure (due to oxygen) and could result in haze depending on the size of the leak, Therefore a leakage check in the CVD is an important step before making an experiment [43]. After pumping the reaction system for a whole day, closing the outlet valve of the chamber, the pressure-increasing rate was measured at a fixed period of time in the chamber to obtain the leakage rate. For this LPCVD system, the leakage rate deviated from 0.13 to 2 mTorr/min, depending on the chamber condition a very low leak rate for a new chamber and higher leak rate for a chamber after long time in service. However, the leakage rate in the system was basically good.

3.3.2 Calibration of Gas Flow System

CVD reactors and other process systems require that the rates of introduction of the process gases into the process chambers be controlled. In some applications, this is achieved by adjusting the gas influx to maintain a constant chamber pressure. More commonly, the process gas flow is directly controlled. To do this, mass flow controllers

are used. Mass flow controllers consist of a mass-flowmeter, a controller, and a valve. They are located between the gas source and the chamber, where they can monitor and dispense the gases at predetermined rates. The operation of a thermal mass flowmeter relies on the ability of a flowing gas to transfer heat. The mass flowmeter consists of a small sensor tube in parallel with the larger main gas flow tube. A heating coil is wrapped around the sensor tube midway along its length, and temperature sensors are located upstream and downstream of the heated point. When the gas is not flowing, and the heat input is constant, the temperatures at both sensors are equal. Flowing gas causes the temperature distribution in the sensor to change. It can be shown that the mass flow, m_f, is given by:

$$m_f = (\kappa W_h \Delta T)^{1.25}$$

Where W_h is the heater power, ΔT is the temperature difference between the points where the sensors are located, and κ is a constant that depends on the heat transfer coefficients, the specific heat of the gas, the density of the gas, and the thermal conductivity of the gas. Mass rate can be thus measured by the temperature difference.

Gas flows were controlled by Applied Materials model AFC 550 automatic N_2 mass flow controllers, which were, corrected for NH3 flow. The pressure in the reactor was measured with a barratry gauge from MKS. The N_2 calibration of the AFC was checked by delivering a fixed volume of gas (product of the metered flow rate and time) into the known reaction chamber volume. The pressure increase was measured and used to calculate the volume of the gas corrected to the standard condition. (25°C, 1 atm).

According to the gas law, the flow rate corrected to STP (sccm) is given by the formula below:

$$\text{Flow Rate} = 60(\Delta P/\Delta t)(T_0 V/P_o T)$$

Where ΔP = pressure increase in Torr,

T_0 = 273 K,

P_0 = 760 Torr,

V = volume of the chamber, cm^3, and

Δt = time of delivering gas, sec.

Routine flow rate calibrations were conducted before every run.

3.3.3 Calibration of Vapor Phase Flow Controller

The TEAB flow controller worked on the principle of measuring the gradient in pressure due to the flow i.e., it uses the combination of Hagen-Poiseuille's principle and the ideal gas law for the measurement of flow.

$$PV = nRT$$

$$\Delta n/\Delta t = V/RT(\Delta P/\Delta t)$$

Where: P = Pressure of the reactor chamber,

R = Universal gas constant,

T = Temperature of the chamber,

n = number of moles of the gas,

The reactor was maintained at room temperature. The volume of the reactor was calculated from the dimensions of the tube. By measuring the rate of pressure increase inside the reactor, the molar flowrate was calculated from the equations above. Once the molar flowrate of the vapor has been calculated, the volumetric flow rate of the gas at standard conditions i.e., in sccm was calculated using the equations given above.

3.4 Deposition Procedure

Boron nitride films were deposited on 3 different types of substrates. Firstly (100) oriented single crystal p-type, boron-doped single-side polished Si wafers (obtained from Silicon Sense Inc.), secondly (100) oriented single crystal p-type, heavily doped with boron single-side polished Si wafers (also obtained from Silicon Sense Inc.) and lastly fused quartz wafers (obtained from Hoya, Japan). The details of the Si wafers are given in Table 3.1. Apart from the substrates, the boron nitride films were also deposited on Platinum and Hafnium carbide films, which in turn were deposited on (100) p-type Si by Sputtering.

The wafers are labeled and accurately weighed (up to 4 decimal places) using an electronic balance. These wafers are then placed on a quartz boat. The wafers used to measure the stress on the film are placed back-to-back at a distance of 12.5 cm from one end of quartz boat and the quartz wafer at a distance of 4 cm from the stress monitors in all the experiments. The boat was placed in the reaction chamber at a distance of 54 cm from the loading end.

Once the wafers are loaded, the door of the reactor is shut and all the inlet valves are closed. Now the bypass valve is opened and the chamber pressure is reduced from atmospheric pressure to 5 Torr. Then the outlet (main) valve is opened and pressure is dropped down to as low as 10 mTorr. This two step procedure of reducing the chamber pressure ensures that the process wafers are not subjected to a sudden force and as a result they don't break. A low pressure is maintained inside the chamber using the vacuum pumps. The furnace is turned on and the required temperature is set. The reactor is then subjected to a baking period till the out gassing rate is very low. The average bake out time was found to be approximately 3 hours. TEAB vapors were sent into the reaction chamber through the vapor phase flow controller and Ammonia was added into the reaction chamber by means of the mass flow controller. Time of deposition was varied according to the required film thickness. Among the deposition parameters recorded were the background pressure, reaction temperature, flow rates of the reactants and the deposition time. Experiments were performed to change the stoichiometry of deposited films by adding ammonia to the amine complex in the reactor.

Table 3.1 Specifications of the Si wafer

Property	Type - 1	Type - 2
Source	Silicon Sense Inc.	Silicon Sense Inc.
Diameter	100 mm	100 mm
Orientation	<100>	<100>
Thickness	525 ± 25 μm	525 ± 25 μm
Type/Dopant	P/Boron	P/Boron
Resistivity	1 - 15	0.01 - 0.02
Grade	Test	Test

Samples were allowed to cool to room temperature and the wafers were removed from the reactor by introducing nitrogen to fill the vacuum chamber and raise the pressure to atmospheric pressure. The samples were then weighed and the deposition rate was calculated by knowing the mass gain (mg/hr) due to deposition. Samples were observed in an optical microscope for the presence of microcracks and for gas phase nucleation.

3.5 Characterization of Boron Nitride Films

3.5.1 Thickness

Film thickness was measured by Nanospec interferometer that bases its estimation on the monochromatic light interface fringes formed within a zone limited by sample surface and a semi-transparent mirror. The device consisted of Nanometrics Nanospec/AFT microarea gauge and SDP-2000T film thickness computer. The thickness of the film deposited on the wafer was measured at five different points. The refractive index provided was first estimated, as for silicon dioxide, 1.46 is the typical value. Thickness was measured at five different points on the wafer. As a checkpoint for the thickness values, the thickness was also measured using the Surface Profilometer having a Dektak probe. Deposition rate was determined as the film thickness over the deposition time, and averaged over all the wafers in the run.

3.5.2 Refractive Index

The refractive index was determined by a Rudolph Research Auto EL ellipsometer, which consists of a polarizer and a compensator. Plane (45°) polarized light the polarizer is elliptically polarized when it passes through the compensator. It is then reflected by the sample surface, collected by a detector, analyzed for its intensity, and finally quantified by a set of delta psi values. The values were then fed to a computer that numerically solves the equation to give the refractive index of the film. The refractive index of the film deposited on the wafer was measured at five different points and then averaged out to the refractive index of the wafer.

3.5.3 Infrared Spectra

Fourier transform infrared (FTIR) spectra of the films obtained from Perkin - Elmer 580 were observed for B-N, B-N-B vibration modes and the presence of N-H, C-H bonding. The levels of interstitial oxygen and phosphorus were determined by using infrared absorption spectroscopy. The analysis was done on a Perkin-Elmer 1600 series FTIR spectrophotometer to determine the characteristics of the deposits. A spectrum of percent transmittance or absorption was obtained for samples of known thickness.

3.5.4 Stress

The stress in the film was determined by a house-developed device, employing laser beam equipment, which measures change in radius of curvature of the wafer resulting

from the film deposited on one side. Two fixed and parallel He-Ne laser beams were incident on the wafer surface before and after deposition. The reflected beams from the two surfaces was then projected by an angled plane mirror as two points onto a scale in a certain distance, and thus, their separation can be measured more accurately. The change in separation of these two points was fed into Stony's Equation to obtain actual stress value. The calculation formula is:

$$\delta = 12.3\ D/T$$

where D = distance difference between two points before and after deposition (mm);

T = thickness of the films, (λm); and

δ = stress of the film (Mpa), negative value indicates compressive stress

3.5.5 X-ray Diffraction

X-ray diffraction patterns were studied to find the structure of the deposited films using IBM PC based Rigaku diffractometer. The analysis of the angular position and intensity of the x-rays diffracted by the material gave the information on the crystal structure and the crystalline phases in the sample. X-ray diffraction occurs when the Bragg requirement is satisfied:

$$n\lambda = 2d\sin\theta$$

Where: λ = X-ray wavelength, d = Interplanar spacing,

θ = Bragg diffraction angle, and n = Order of diffraction.

3.5.6 UV/Visible Spectrophotometer

The optical transmission of the films was measured using a Varian DMS 300 UV/visible spectrophotometer over a range of wavelength from 190nm to 900nm. This also gives an approximate estimation of the optical band gap of the semiconducting BN thin film.

3.5.7 X-ray Photoelectron Spectroscopy (XPS)

X-ray photoelectron spectroscopy was used for the compositional analysis of the boron nitride films. Low energy x-rays of K-alpha aluminum (which has energy of 1.487 keV) were used to cause the photoelectron emission. The principle used here is that just as the electron bombardment of materials can produce emitted electrons and x-rays, striking the material with x-rays can do the same. In this technique, only electrons from the top 1-10 monolayers are emitted without significant loss from collision. Thus even though the x-ray beam penetrates deep into the sample material, XPS is basically a surface analysis technique. However the films were ion milled to a depth of 500Å and then again the analysis was carried out. Hence both the surface as well as the composition in the film were determined by this technique.

3.6 Electrical Characterization of BN Thin Films

3.6.1 Metallization

The electrical properties of the synthesized films were determined by studying the characteristics of the devices made by the films. To study the electrical characteristics of

the device, an electrical contact was provided by Al metallization. The boron nitride thin films were coated with pure Al. This was done in an evaporator, and the important parameters of deposition are given in Table 3.2. A shadow mask was used to obtain Al dots of diameter 300μm and 600μm on the boron nitride film, while a uniform coating of Al is deposited on the back surface (Si surface of the stress monitor).

Table 3.2 Parameters for metallization of BN thin films

Base pressure	10^{-6} Torr
Heating source	Tungsten filament (resistance heating)
Evaporating source	Al wire
Purity of evaporating source	99.9999% (Al)
Rate of deposition	50 Å/min.
Ultimate thickness of deposit	900 Å
Substrate temperature	room temperature
Dist. between the filament and the substrate	200 mm
Size of the dots	300 μm and 600μm diameter

Thin Al films were deposited by applying heat to the source of the film material, thereby causing evaporation. The heated source was resided in a high-vacuum environment, hence the vaporized atoms/molecules are likely to strike the substrate without suffering any intervening collisions with other gas molecules. The rate of mass lost from the source per unit area per unit time, R can be estimated from the Langmuir-Knudsen relation:

$$R = 4.43 \times 10^{-4} (M/T)^{1/2} P_e$$

$$R = 5.83 \times 10^{-2} (M/T)^{1/2} P_e$$

Where: M is the gram-molecular mass; T is the temperature in °K, and P_e is the vapor pressure in Pa.

Al films were deposited with resistance-heated source. That is, a wire of low vapor pressure metal Tungsten was used to support small strips of the metal to be evaporated. The substrate was placed above the source. The chamber was now evacuated and a pressure as low as 10^{-6} Torr was achieved. Now the power supply to the resistance is slowly increased i.e., the W-wire is then resistively heated till Al on the resistance wire melts and evaporates. Once evaporated, the vacuum is broken and the chamber is opened. The substrate coated with the Al film is then removed.

3.6.2 Device Fabrication

Two kinds of devices were built using boron nitride thin films, the MOS (Metal Oxide Semiconductor) and the MIM (Metal Insulator Metal). Further, the MIM structures were built by 2 ways, in the first method a metal film was deposited on the Si substrate and in the second, a very highly conducting Si substrate was used i.e., type - 2 substrate as shown in the table. Platinum and Hafnium carbide were used as the metal to make the MIM structures. Detailed schematics of the fabrication process for the structures are shown in fig.3.2 through fig.3.4.

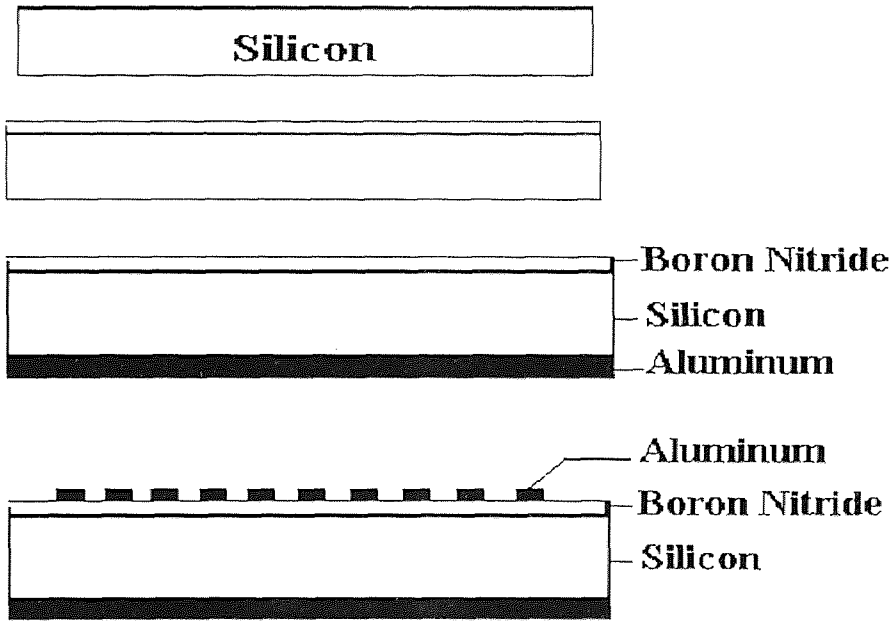

Figure 3.2 Process flow diagram for the fabrication of the MOS device

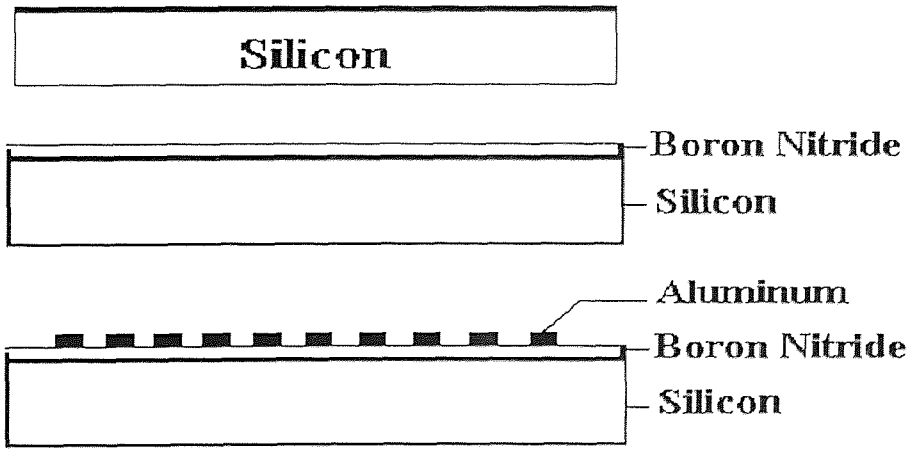

Figure 3.3 Process flow diagram for the fabrication of the MIM device (Si Type-2)

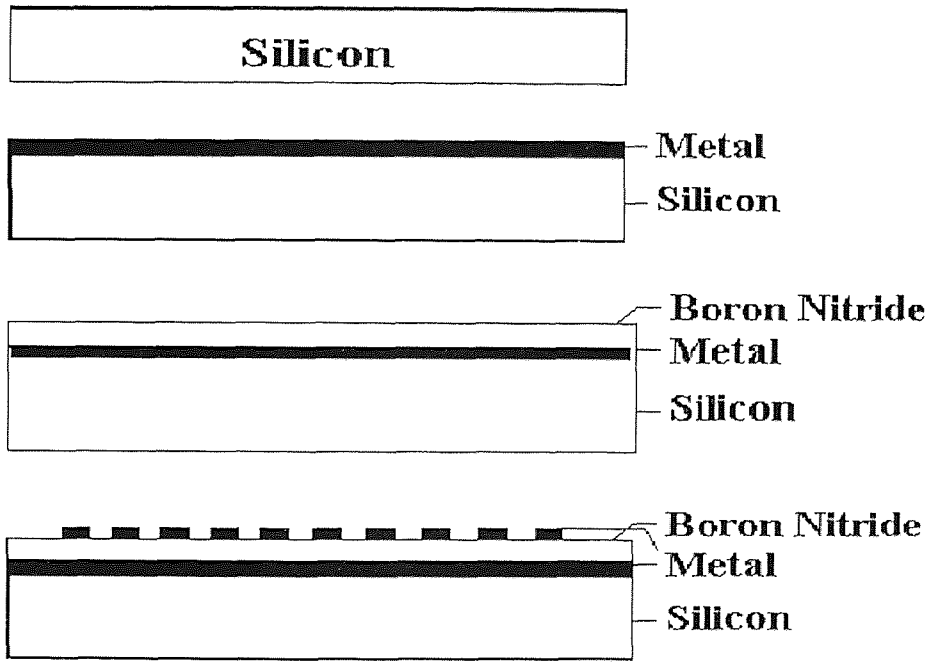

Figure 3.4 Process flow diagram for the fabrication of the MIM device with metal film

3.6.3 Capacitance - Voltage and Current - Voltage Measurements

Capacitance - voltage (C-V) and current - voltage (I-V) measurements were done for the films on both the low resistivity as well as the high resistivity p - type Si substrates. On the front side of BN, Al dots were evaporated through a shadow mask. The backside BN was removed by plasma etching (if necessary) and Al was deposited for back contact as explained in the previous section. The dielectric constant of the BN films were measured at five places and the breakdown voltage was determined. Subsequently, a bias stress study was made by applying a ± 1MV/cm for 2 - 5 minutes at room temperature and C-V measurements were done after each polarity of stress. Temperature-bias stress measurements were also made to find out if there are trapped charges in the insulator. This was done by applying a positive and negative polarity of 0.5 MV/cm for 10 minutes

at 120 °C. To find out the nature of the charges, bias-temperature aging studies were done on the samples. The recombination-generation kinetics of the electrons in the inversion region of the device was studied by taking the C-V measurements with a-c signals at different frequencies. Frequencies ranging from 10 Hz to 1Mhz were used in this study. Also, the mobility of charges and the presence of charge traps were studied by shining of light with different intensities on the devices.

3.7 Overview of Basis of the Present Work

Before going into the findings of the present work, for the sake of completeness and better understanding, a brief review of the research done [44] on the synthesis and characterization of boron nitride thin films over a series of temperatures from 300 °C to 850 °C using TEAB and ammonia as precursors is discussed. Based on these results, further work was done by varying the flow ratio of ammonia and TEAB to study the growth kinetics of the reaction. In figure 3.5, the variation of growth rate of BN as a function of temperature is shown.

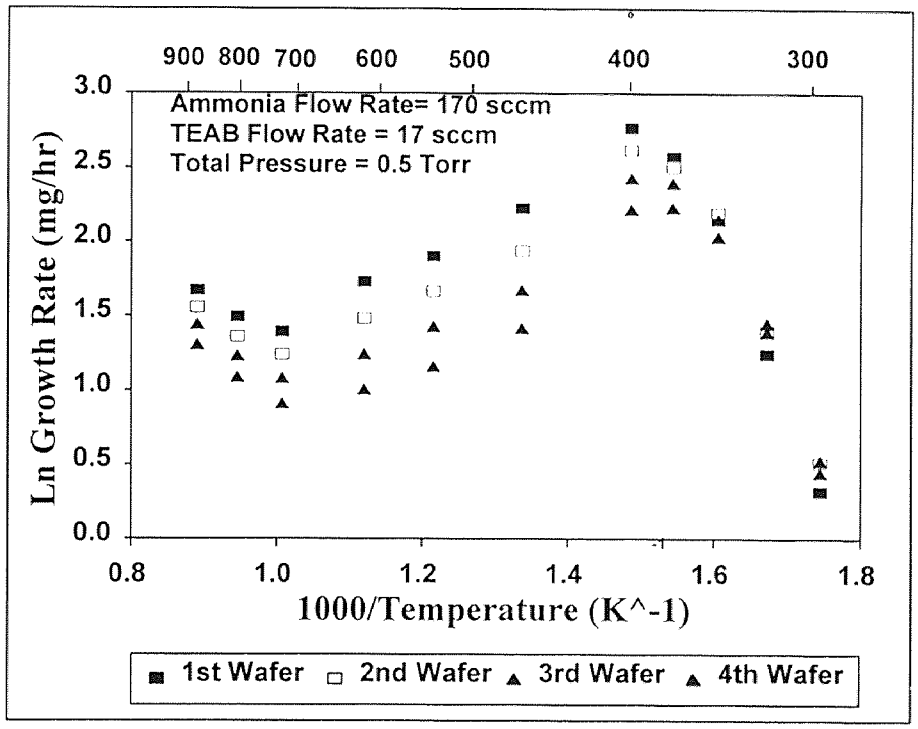

Figure 3.5 Temperature-growth rate relationship for depositing BN thin films on Si wafers

3.7.1 Kinetics of Film Growth

At a fixed total flow rate of 187 sccm, NH_3/TEAB ratio of 10/1 and total pressure of 0.5 torr, the kinetics of film growth were investigated in the temperature range of 300° to 850°C. The deposition rate plotted over the range of 300° to 350°C exhibits an Arrhenius behavior of 22 kcal/mol. The addition of NH_3 lowered the minimum deposition temperature by around 300°C. Between 350° and 400°C, the curve changes slope reflecting the onset of the changes in reaction mechanism. It is observed that at these low temperature region, the reactants did not become sufficiently hot prior to their flow over the substrates: as they travel toward the exhaust they become warmer leading to increased

deposition rates on the last wafer along the flow. In the range between 400°C and 700°C, the deposition rate decreases monotonically due to the increased contribution of depletion effect. Above 720°C, a slight increase in deposition rate is assumed due to the changes in the gas phase chemistry which are also reflected in the changes in the film composition, density, stress, color etc. The shape of the curve is complex and consistent to the curve of the refractive indices reflecting the chemical mechanism of the processes and the composition of the films are strongly dependent on the temperature.

In the present study 3 temperatures were taken from the above graph at 550°C, 575°C and 600°C and the TEAB flow was maintained at 1-5 sccm using a vapor source flow system as explained earlier. The flow rate of NH_3 was varied to obtain ratios of 50:1 for these temperatures.

The effect of flow ratio and temperature with the thickness, density, stress, refractive index, optical absorption coefficient, dielectric constant, I-V, and C-V characteristics were studied.

CHAPTER 4

RESULTS AND DISCUSSION

4.1 Introduction

The results of boron nitride thin films synthesized on Si and quartz substrates at a constant pressure of 0.05 Torr, at 3 temperatures 550°C, 575°C, and 600°C at various ammonia to TEAB flow ratios are described in this Chapter. The deposition time was varied to obtain an average thickness of about 1500Å to facilitate electrical measurements.

The films appeared light brown to golden yellow on quartz wafers and were reasonably transparent. A more detailed description of the optical transparency and the absorption coefficient of the film is described later in this Chapter. There were no cracks on the film surface and consistently, in all films the thickness varied by about 100Å at the bottom - near the primary flat of the Si wafer and at the top (the top being thicker). However the films were uniform over majority of the substrate. When observed under the optical microscope, no traces of gas phase nucleation could be observed.

In the subsequent sections the characterization of films in terms of IR, UV and visible absorption spectroscopy was done to understand the nature of the bonding and contamination of films if any, identified by impurity peaks in the spectra. X-ray photoelectron spectroscopy analysis was also done to find out the exact composition of the film. The effect of flow ratio and temperature with the thickness, density, stress, refractive index and optical absorption coefficient are discussed. Finally, the electrical characterization of the films is discussed.

4.2 Kinetic Study of Boron Nitride Deposition by LPCVD

The synthesis of films produced using TEAB with NH3 has been investigated in this study. At a fixed TEAB complex flow rate of 1 sccm and total pressure of 0.05 Torr, the

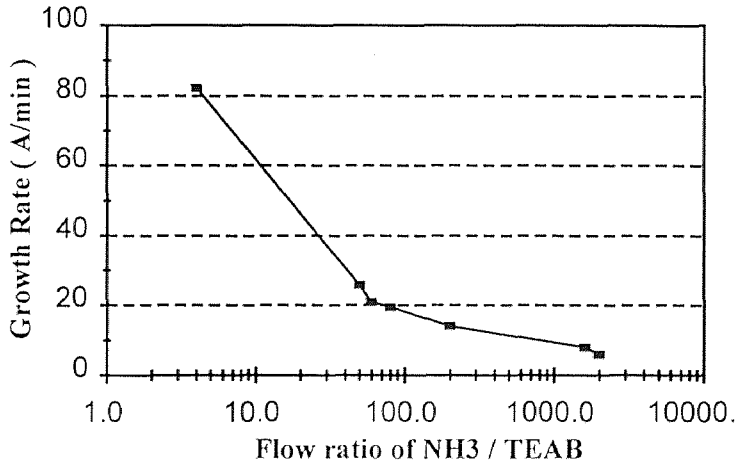

Figure 4.1 Variation of growth rate with the flow ratio of the reactants.

growth rate is shown in Fig. 4.1 and Fig. 4.2. For the deposition temperature range of 550 to 600 °C, the growth rate was found to decrease with increasing temperature due to the combination effects, including the transition into the mass-transfer limited regime and adsorption of decomposition products which act as retardants to the growth process. The growth rate decreases monotonically due to the depletion of reactants caused by the reactions on the hot wall of the furnace. A plot of growth rate as a function of the flow ratio is shown in Fig. 4.1. It is observed that as the ammonia flow increases, the growth rate decreases rapidly and approaches a plateau at around 300 sccm. The higher presence

of ammonia may results in filling up the surface sites, which dilutes the TEAB and thus accounting for the reduced growth rate.

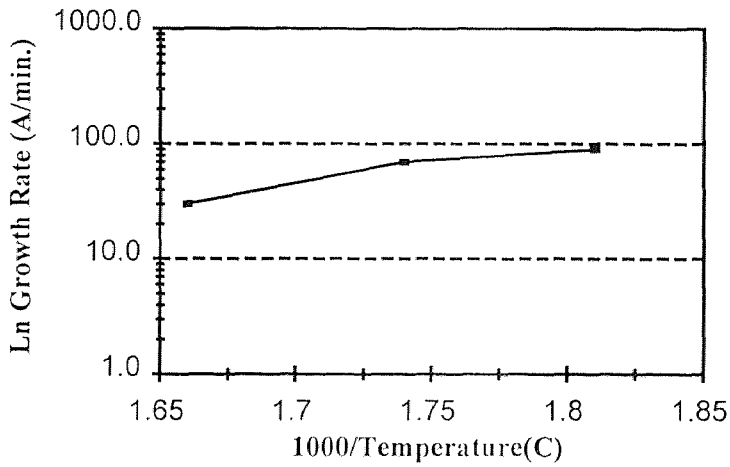

Figure 4.2 Variation of average growth rate as a function of temperature

4.3 FTIR Spectroscopy and XPS Analysis of BN Thin Films

The typical FTIR absorption spectra of boron nitride thin films (Figure 4.3(a)) at 400°C, 0.5 Torr pressure and a flow ratio of NH3/TEAB = 10/1 showed absorption peaks at wavenumber of about 1350 cm^{-1} corresponding to the B-N vibration mode, and a small peak close to 800 cm^{-1} corresponding to the B-N-B vibration. Apart from these major peaks, B-H peak at wavenumbers 2500 cm^{-1}, and N-H peaks at wavenumbers 3200 cm^{-1} and 3400 cm^{-1} C-H peak at 2900 cm^{-1} could be seen. Also a contamination O-H peak can be seen at about 3600 cm^{-1}.

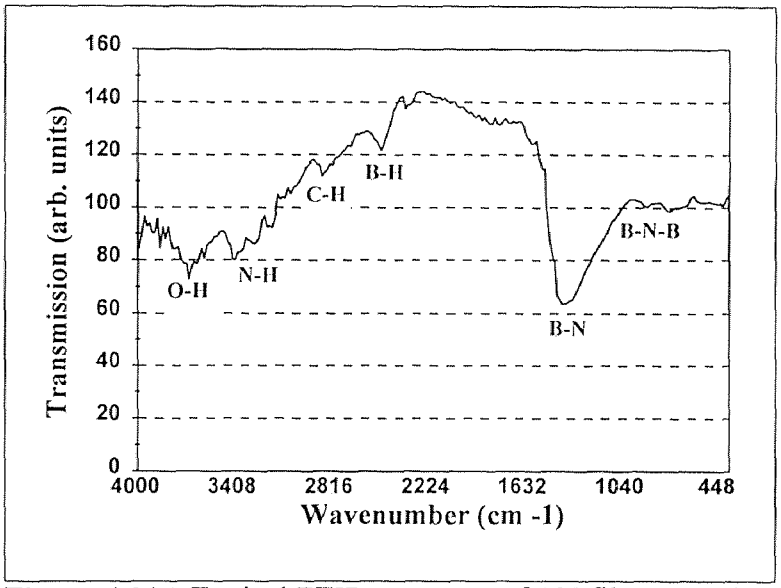

Figure 4.3(a) Typical FTIR spectrum of BN films at 400°C

It can be seen that the B-N and B-N-B absorption peaks increase with increasing flow rate of ammonia at all the temperatures under consideration. In addition, with increase in temperature, at 550°C (Figure 4.3(b)), the peaks at wavenumbers 3400 cm^{-1}, 3200 cm^{-1}, and 2900 cm^{-1} and 2500 cm^{-1} corresponding to N-H, C-H and B-H vibration modes respectively disappear.

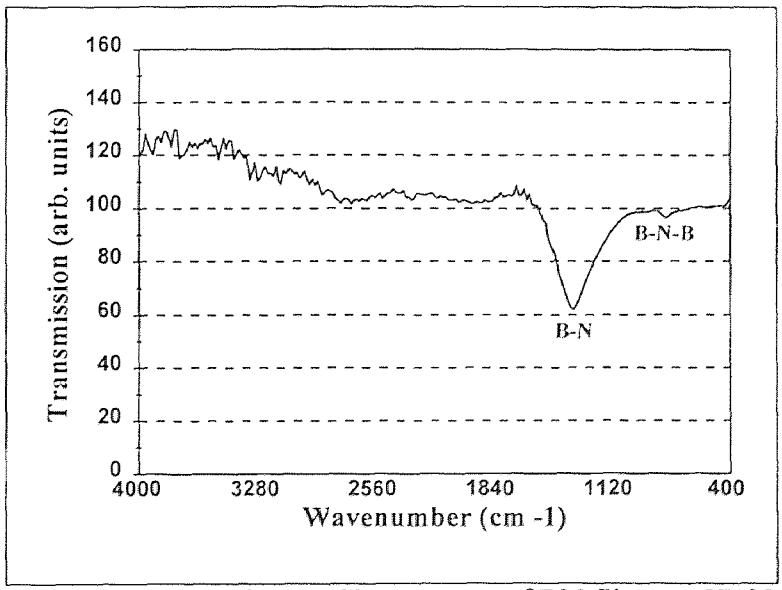

Figure 4.3(b) Typical FTIR spectrum of BN films at 575°C

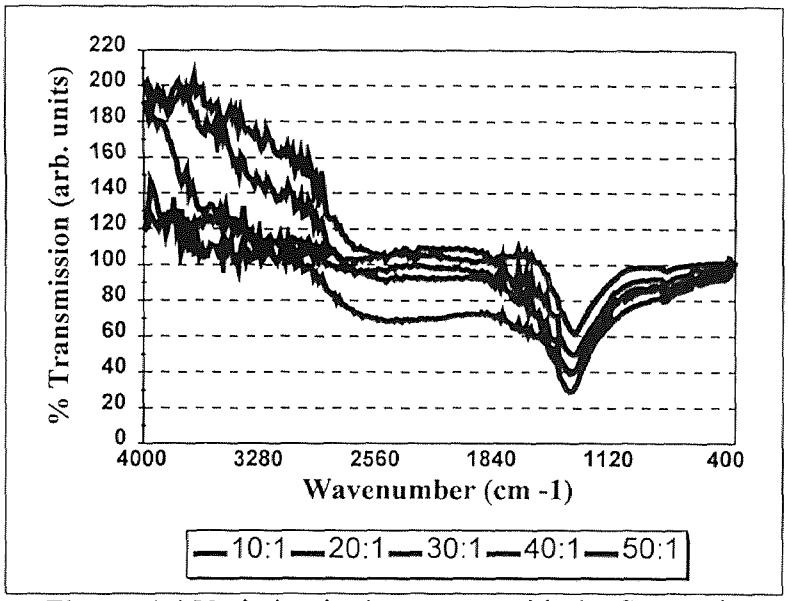

Figure 4.4 Variation in the spectra with the flow ratio

Figure 4.3(b) shows the shift in the peak position with increasing temperature at a constant flow ratio of NH_3/TEAB = 50/1. This indicates that the stoichiometry of the film is changing with increasing flow ratio. As the thickness increases, the intensity of the peak also increases. XPS analysis indicated a carbon percentage of about 8, but from the infrared absorption spectra, no C-C or C-H peaks at high temperatures and at high flow rate could be identified. This reveals that it is not bonded in any carbide form, rather in an elemental form. Thus, FTIR is insensitive to the presence of carbon in the film. Thus the film is essentially amorphous carbon containing boron nitride.

4.4 UV/Visible Spectroscopy of BN Thin Films

The optical transmission of the boron nitride film deposited on quartz wafers was studied using a UV/Visible spectrophotometer. Typical optical transmission curve is shown in Figure 4.5.

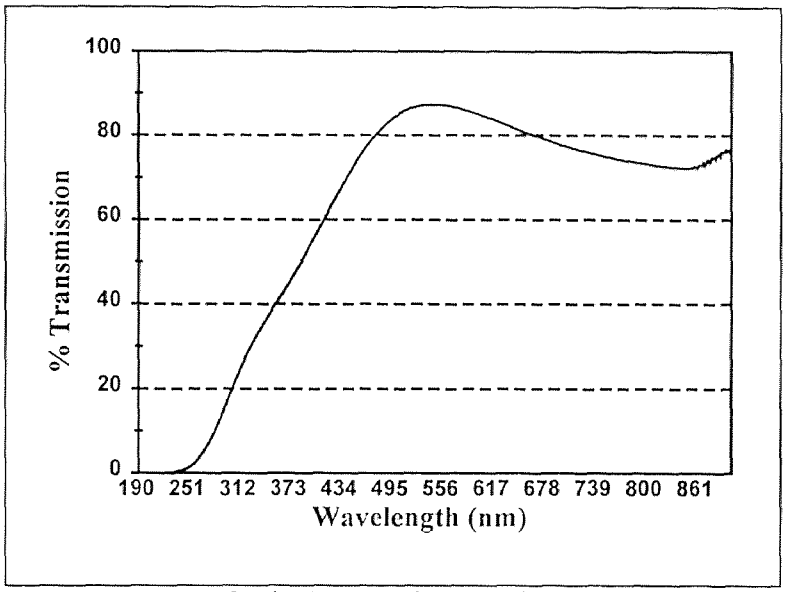

Figure 4.5 Optical transmission of BN thin films

The optical transmission of the films synthesized varied from 92% to 72% at 633nm (corresponding to red light) depending on the thickness of the film and the stoichiometry of boron, nitrogen and carbon ratios in the films. As the wavelength is reduced from the visible region to the ultra violet region (approx. < 300nm) the transmission goes down and at about 210nm the light is completely absorbed. This is typical of a semiconducting material with the electrons jumping from the valence band to the conduction band as a result of the excitation of the electrons due to this supplied quanta of energy (by a photon). The optical band gap of this semiconducting material was estimated to be 4.167 eV.

4.5 Structure Study

In the case of synthesis of BN thin films, a heterogeneous reaction must occur in order to obtain good films. However, some portions of the overall reaction may occur in the gas

phase. BN molecules adsorbed on the Si wafer surface diffuse randomly and have a greater opportunity to re-evaporate (desorb) because they are less firmly bound to the surface. As the adsorbed molecules diffuse on the surface, they may encounter other diffusing molecules and form a pair. This molecule pair would be more stable than an isolated molecule and would less likely to desorb. As the pairs diffuse on the surface, they may join other molecules, forming a larger and more stable cluster, until the cluster had a low probability of desorbing and a critical cluster or stable nucleus was formed. The probability of diffusing molecules encountering each other depends strongly on the number of adsorbed molecules on the surface. Thus, it is a strong function of their arrival rate (through the pressures of the precursors) and their desorption rate (through the temperature of substrate and the binding energy of the diffusing molecules to exposed surface). After stable deposited nuclei formed, additional adsorbed molecules diffusing on the surface can either initiate additional nuclei or join existing nuclei. When the existing nuclei were close enough together, additional molecules were more likely to join an existing nucleus, and the number of nuclei saturated and remained constant as the size of each nuclei grows. The saturation number of nuclei depended on the substrate, the arrival rate of molecules, and the temperature. Thus, a continuous film formed as the nuclei impinged on each other. Ever after a continuous film formed, the structure was strongly influenced by the thermal energy available for surface migration. At very low temperatures, the adsorbed BN molecules had little thermal energy and cannot diffuse significantly on the substrate surface before they were covered by subsequently arriving

molecules. Once they were covered, their random arrangement was locked into place, and an amorphous structure with no long-range order formed. At higher temperatures, adequate surface diffusion was possible to allow a crystalline structure to form [20].

The X-ray diffraction pattern of BN films deposited on silicon at the highest deposition temperature of 575 °C (shown in Figure 4.6) only exhibits the peak of Si (100) at about 69 °, the peaks of BN are not present. Therefore, the films are amorphous at all temperatures that were studied.

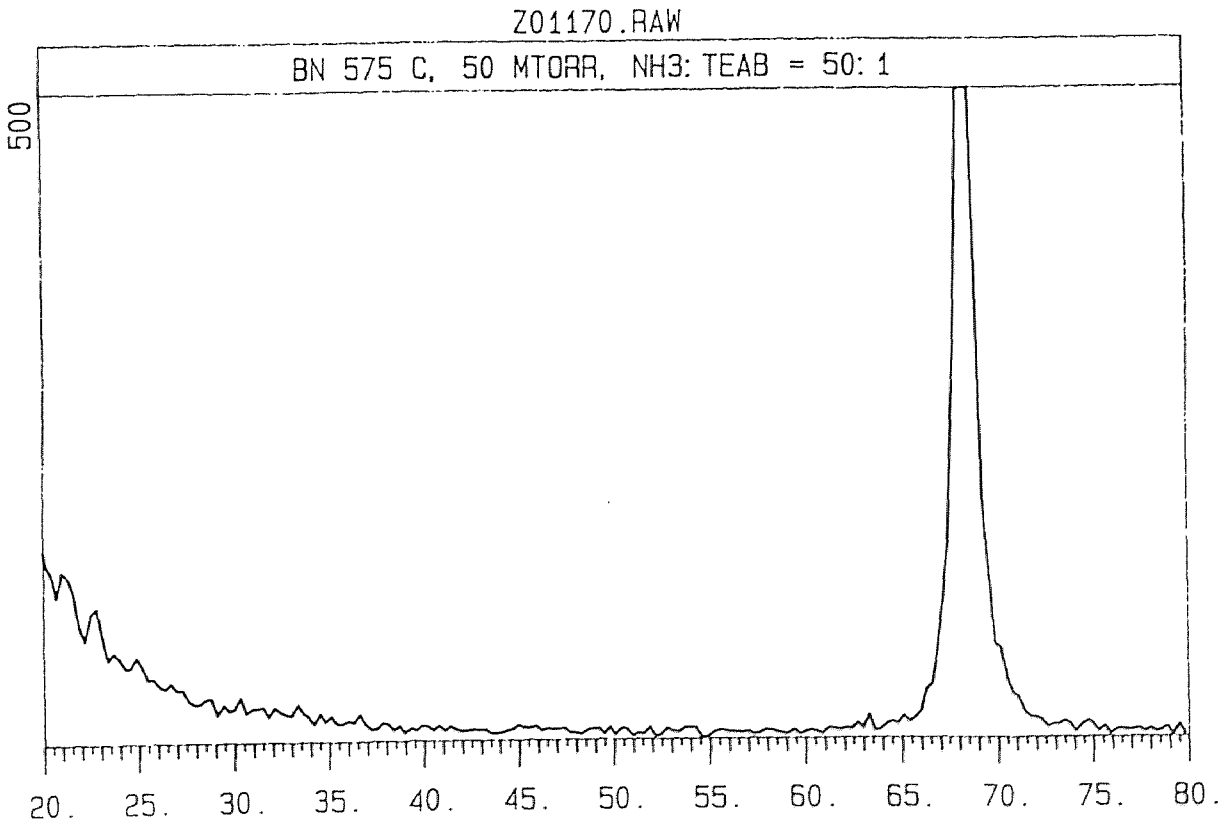

Figure 4.6 X-ray diffraction pattern for a boron nitride film on silicon deposited at a temperature of 575 °C, pressure of 0.05 Torr, TEAB flowrate of 1 sccm, and NH_3 flowrate of 50 sccm.

4.6 Effect of Flow Ratio of NH_3/TEAB

4.6.1 On Film Thickness

In all cases the film thickness was maintained at about 1500 Å to facilitate the electric characterization viz., the I-V characteristics as well as dielectric constant measurements. To this effect, the time of deposition was varied.

In all the cases, there was higher deposition rate in the stress monitor facing the loading end - also the entry of the precursors - and lower deposition rate in the wafer facing away from the loading end in the stress monitors. At lower flow rates of NH_3/TEAB, the thickness' of the stress monitors are comparable but, with increasing ammonia flow, the depletion effect is much more predominant.

4.6.2 On Film Density

The density of the films was determined by dividing weight gain by film volume as calculated from the product of film thickness and known area of the wafer. The thickness' used were based on the values obtained by the Nanospectrophotometer. It is seen that the density decreases with increase in flow ratio of ammonia/TEAB (Figure 4.7). This could be a result of more porous films. However, gas phase nucleation could not be seen in the optical microscope. As seen from the XPS study, the presence of carbon makes the refractive index measurements and hence the thickness measurements difficult. Hence the reason for low density could not be explained with certainty. However, in most LPCVD processes, there is a variation of the density of the film is common due to the non-stoichiometric films.

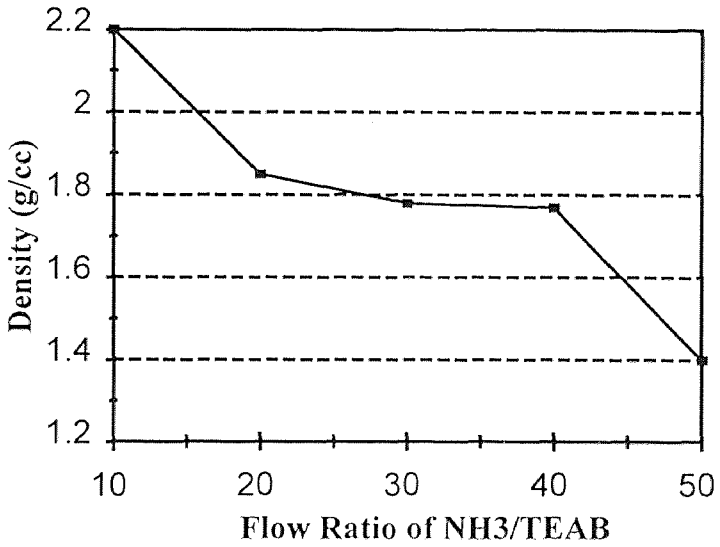

Figure 4.7 Variation of film density with increasing flow ratio of NH_3/TEAB

4.6.3 On Refractive Index

Figure 4.8 shows the variation of the refractive indices of the film with the flow ratio. With increase in the ammonia flow rate, the refractive index increases. The increase is marginal though and the indices hover around 1.8 to 2.0. Interestingly, when the flow ratio was increased drastically at 550°C to 40:1 and 50:1, the refractive index dropped to 1.59. This could be due to the attainment of stoichiometry of boron and nitrogen with a consistent amount of carbon in the film (about 8%) and negligible oxygen.

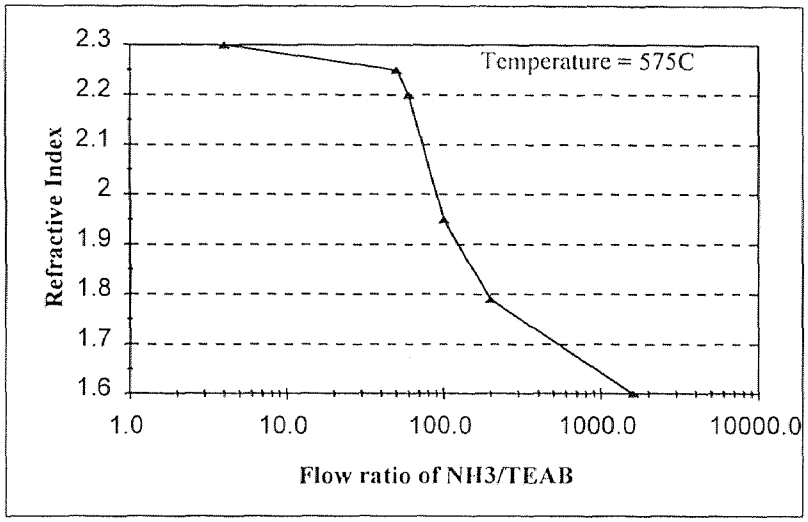

Figure 4.8 Variation of refractive index with increasing flow ratio of NH_3/TEAB

4.6.4 On Film Stress

At lower flow ratios of 10:1 of NH_3:TEAB (Figure 4.9), the films were mildly tensile and the values are comparable (about 50MPa). With increase in the ammonia flow rate, the stresses in the film changed from mildly tensile to mildly compressive and the trend

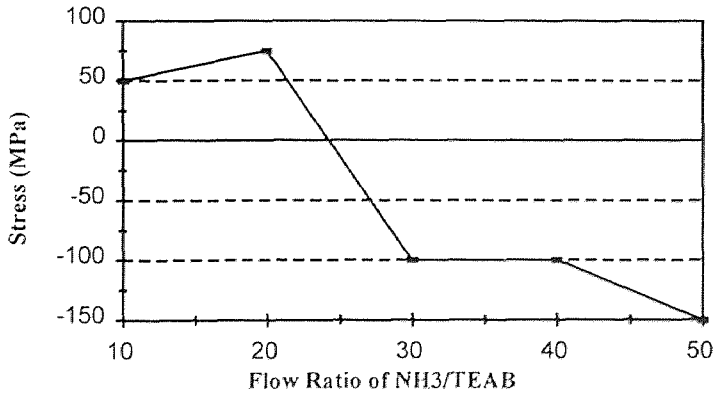

Figure 4.9 Variation of stress with increasing flow ratio of NH_3/TEAB

continued at higher flow ratios of 50:1 at 550°C. Within the temperature ranges studied the highest compressive stress attained was about 150 MPa. The effect is mainly due to the influence of ammonia which increases the nitrogen percentage in the films since the carbon percentage is almost constant over this range of temperature.

4.6.5 On Optical Transmission

Optical transmission measured using a UV/visible spectrophotometer is described earlier in this Chapter. The transmission was studied at a wavelength corresponding to red light (λ = 6330Å). The absorption coefficient α was calculated using Beer-Lambert law

$$I/I_o = \exp(-\alpha x)$$

where I/I_o is the fraction of the transmitted light and x, the thickness of the film.

All thicknesses were normalized to 1 cm and the absorption coefficient was calculated. It was seen that near stoichiometric BN films are reasonably optically transparent.

4.7 Effect of Temperature

4.7.1 On Film Thickness

The thickness of the film constantly decreases with increase in temperature consistent with the growth kinetics as shown in Figure 3.2 [42]. The monotonic decrease in growth rate is due to the depletion of reactants caused by reactions on the hot walls at the front of the furnace. Evidence for that depletion is seen in the variation of thickness in the front and rear wafers of the back-to-back stress monitor Si wafers. The results is in agreement

with the results of Adams et al.[20] for reactions involving diborane and ammonia where severe depletion effects were seen in the same temperature regime.

Borane is generally considered to be the principal factor controlling the growth rate [20,38], its depletion with increase in temperature is reflected in both the growth rate as well as the film composition. Figure 4.12 shows the effect of depletion of the stress monitors with increase in temperature. At 400°C, the depletion is less but with increasing temperature the thickness of the wafer in front is almost double that of the one behind it. The depletion was more at higher temperatures (Figure 4.12). This is consistent with the results obtained by Levy et al. [44] showing depletion at temperatures of 550°C and less depletion at 400°C.

4.7.2 On Film Density

At lower flow ratios the films are denser and with a constant flow ratio of NH_3/TEAB = 10/1, with increase in temperature the films tend to become denser. But as the flow ratio of NH_3/TEAB is increased, the density decreases, probably resulting in porous films or as discussed earlier, the presence of carbon present in the films could have led to erroneous reading in the ellipsometer. In all, the density of films were comparable.

4.7.3 On Refractive Index

With increase in temperature the refractive index decreased and this is consistent at the 3 temperatures studied. This is due to the tendency of the film towards stoichiometric boron nitride composition.

4.7.4 On Film Stress

At lower temperatures and low ammonia flow rate the films were mildly tensile and the films became more tensile with increase in temperature. while at higher flow ratios and lower temperature, the films were mildly compressive and the compressive stress increased with increase in temperature. Interestingly, a transition from mildly compressive to mildly tensile behavior with increase in temperature was seen in the films at a constant NH_3/TEAB ratio of 20:1.

4.8 Electrical Characterization of BN Films

A detailed electrical characterization was done to determine the potentiality of the films as low ε IMD. CV and IV measurements were done for the films on both the type-1 and type-2 substrates. MIS and MIM structures were fabricated to study the CV and IV behavior exhibited by the films. The following table gives the summary of the electrical measurements carried out on the boron nitride films.

Table 4.1 Electrical data measured for BN films

Substrate	Thickness (Å)	Dielectric constant
type 1-Si	1500	3.5 - 4.5
type 2-Si	1500	3.5 - 4.5

4.8.1 Dielectric Constant Measurements

The dielectric constant of BN films measured at five locations on every sample was in the range of 3.2 to 3.4. The breakdown voltage was more than 4 MV/cm which is the

equipment limit. The dielectric constant was found to be frequency dependent and was measured at different frequencies ranging from 1KHz to 1MHz by a HP4194A CV/IV measuring instrument. The dielectric constant ε was measured using the formula

$$\varepsilon = Cd/A$$

where d is the thickness of the film, A the area of the capacitor (area of the Al contacts - 300μm and 600μm) and C is the effective series capacitance of the dielectric as well as the intrinsic capacitance generated due the applied potential on the minority carriers of the dopant of the Si wafers. The latter varies with changes in applied voltage across the Al contacts. Typical CV plot obtained for BN films on the HP4149A is shown in fig 4.10.

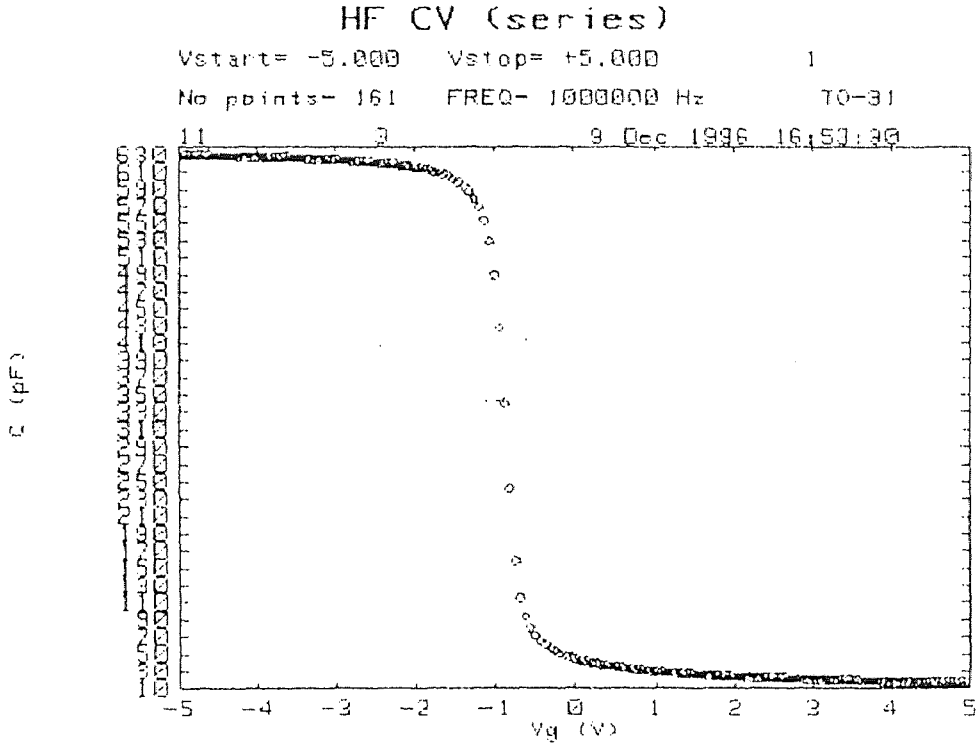

Figure 4.10 Typical MIS capacitance-voltage curves for LPCVD boron nitride

In describing this curve we begin at the left side (negative voltage), where we have an accumulation of holes and therefore a high differential capacitance of the semiconductor. As a result the total capacitance is close to the insulator capacitance. As the negative voltage is reduced sufficiently, a depletion region that acts as a dielectric in series with the insulator is formed near the semiconductor surface and the total capacitance decreases. The capacitance decreases until finally inversion is reached. With inversion there is no further change in the capacitance, since the depletion width has reached its maximum.

4.8.2 Investigation of LPCVD BN-Si Surfaces using MIS Structures

The exact nature of the BN-Si interface is not yet fully understood. The MIS characteristics is greatly influenced by the interface traps and the oxide charges that exist. Hence the properties of the BN film can be studied by an investigation of the MIS structure having BN as the insulator. The basic classifications of the traps and charges are as follows:

1. Interface trapped charges,
2. Fixed oxide charges,
3. Nitride trapped charges and
4. Mobile ionic charges

An interface trap is considered as a donor if it can become neutral or positive by donating an electron. An acceptor interface trap can become neutral or negative by accepting an electron. When a voltage is applied, the interface-trap levels move up or down with the valence and the conduction bands while the fermi level remains fixed. This change of

charge contributes to the MIS capacitance and alters the ideal MIS curve. In other words, the interface trap exhibits a frequency dependent behavior. Hence the presence of interface traps may be detected by the frequency dependent study of the MIS structures. The result of such a study is shown in the fig. 4.11.

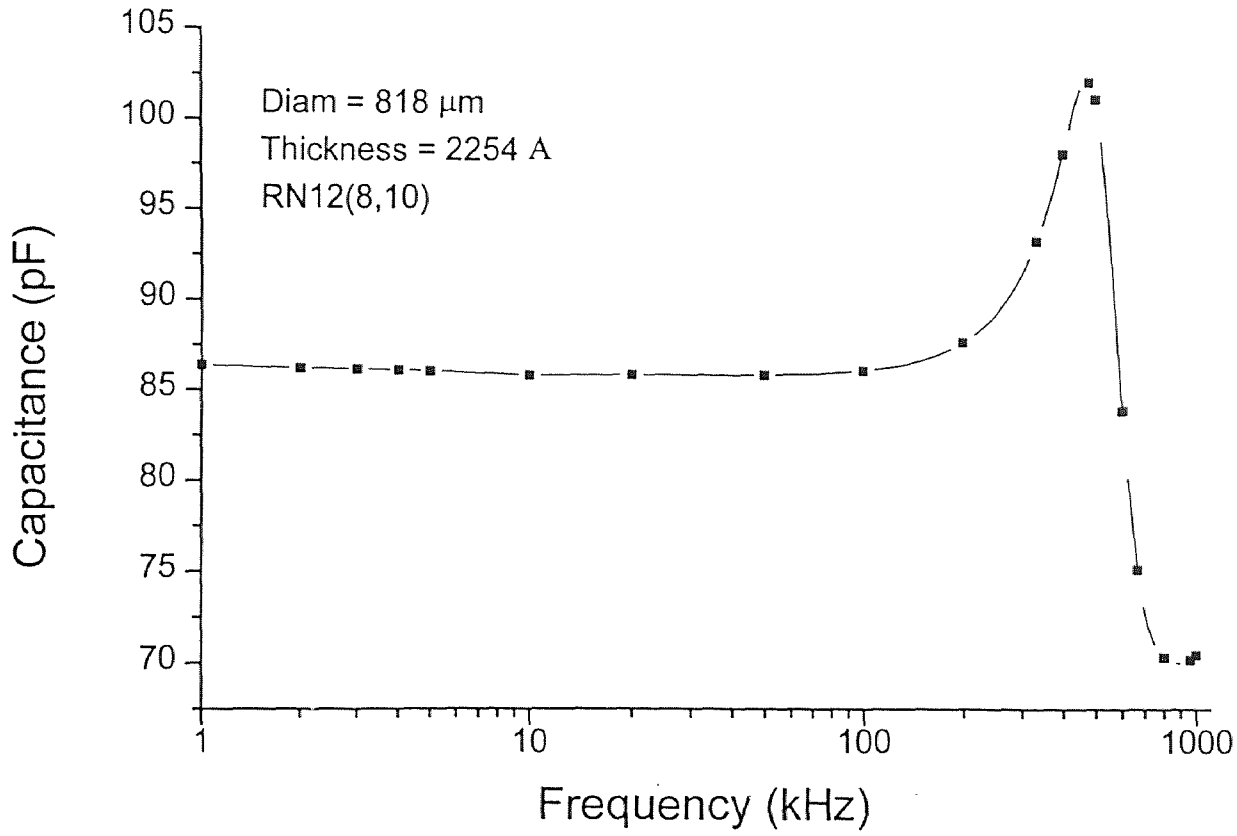

Figure 4.11 Capacitance-frequency plot for BN MIS structures

From the fig. 4.11 we can see that as the frequency is increased, the accumulation capacitance decreases. The reason being, at high frequencies the interface traps cannot follow the ac voltage swing, which yields a capacitance free of the interface traps. Hence we can conclude that the MIS structures which were fabricated contained significant

density of the interface traps. This could be one of the reasons for not achieving lower dielectric constants.

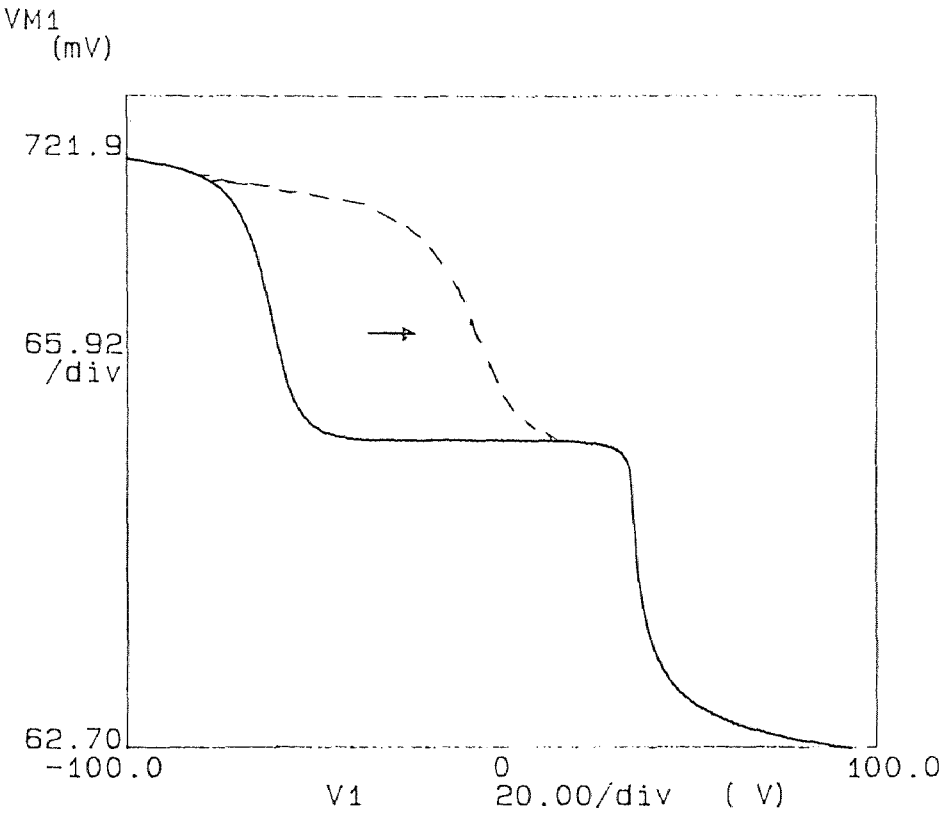

Figure 4.12 C-V curve shift along the voltage axis due to (+) or (-) fixed oxide charge

The fixed oxide charge has the following properties: It is fixed and cannot be discharged or charged over a wide variation of the surface potential; it is located within the order of 30 Å of the Si-SiO2 interface; its density is not greatly affected by the oxide thickness or by the type or concentration of the impurities in silicon; it is generally positive and depends on oxidation and annealing conditions, and on the silicon orientation. The presence of fixed charge would cause a shift in the C-V curve, in

accordance with the principle of charge neutrality. The presence of ionic charges like sodium also causes the shift of the C-V curve because these ions are free and can move back and forth through the film, depending on the biasing situation. Also the presence of the nitride trapped charge causes the C-V curve shift. These traps are associated with the defects in the film. They are usually neutral, and are charged by introducing electrons and holes in the film. Once charged, for the same surface potential, the applied voltage would be reduced indicating a shift in the C-V curve.

Fig. 4.12 shows significant shift in the C-V curve suggesting the presence of a good number of a combination of fixed oxide charges, ionic charges and nitride trapped charges.

Bias temperature cycle not only indicated the presence of mobile ions, it also shows the presence of trapped positive charges in the bulk of the insulator. Although some of the trapped negative charges can be discharged in the gate or in the semiconductor, the trapped positive charges are essentially immobile on this field and temperature range. These trapped charges could be due to the dangling bonds caused by the following 2 reasons:

1. the boron rich nature of this non-stoichiometry of the films
2. the elemental carbon in the films.

These two facts is already shown in the XPS analysis. Low precursor ratio yielded boron rich films whereas high substrate temperatures caused the unbonded excessive carbon.

CV shift in response to the polarities indicates a presence of mobile ions in the insulator. Third, there is considerable trapped immobile charges in the bulk of the

insulator for which the flat-band does not go back to the original value prior to the aging. Fourth, the possibility of trapped negative charges being attracted to the gate electrode or to the semiconductor and consequently being discharged cannot be excluded.

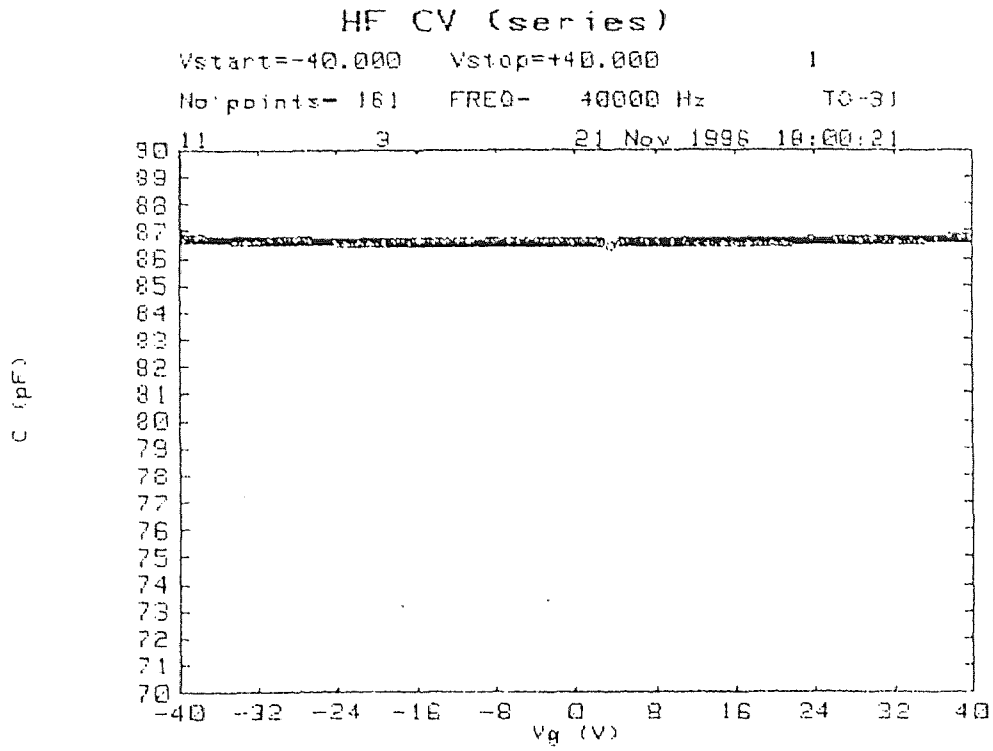

Figure 4.13 Capacitance-Voltage measurements on MIM structures

It is seen that in all the cases the dielectric constant of the films increased with increase in flow ratio. This could be due to the varying stoichiometry in the films, or the variation of thickness of the film or could be due to the effect of carbon impurity in the

boron nitride film. The least value obtained was 3.12 at a deposition of 575°C, pressure of 0.05 Torr and a flow ratio of NH_3/TEAB = 50/1. From the XPS analysis also it is seen that the films tend to attain stoichiometry and more transparent films at these deposition conditions.

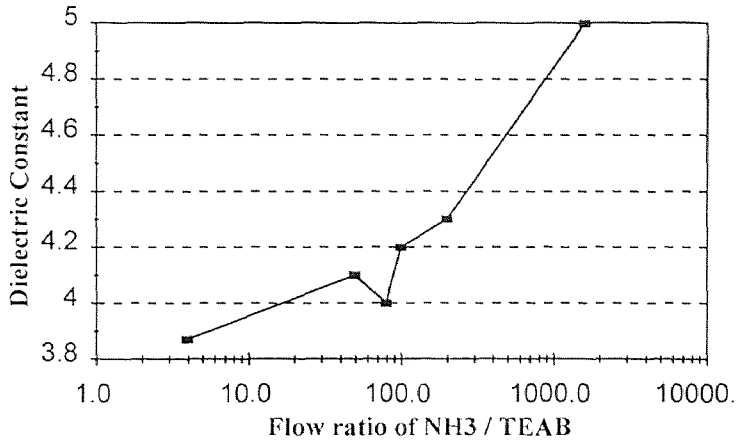

Figure 4.14 Variation of dielectric constant with flow ratio of NH_3/TEAB

A dielectric constant reacts to electromagnetic radiation differently from free space because it contains electrical charges that can be displaced. For a sinusoidal electromagnetic wave, there is a change in the wave velocity and intensity described by the complex coefficient of refraction

$$n^* = n - ik$$

where n is the index of refraction and k is the index of absorption. The coefficient of refraction is related to the complex dielectric constant $(n^*)^2 = \varepsilon^* = \varepsilon' - i\varepsilon''$, where ε' is the relative dielectric constant and ε'' is the relative dielectric loss factor. Neglecting the imaginary terms, the dielectric constant is equal to the square of the index of refraction.

$$\varepsilon = n^2$$

Thus by knowing the refractive index of the film, a fairly good idea of the dielectric constant of the material can be estimated.

4.8.3 Current-Voltage (I-V) Characteristics of the Films

Fig. 4.15 (a)/(b) shows the I-V characteristics of BN films deposited on type-1 and type-2 Si wafers respectively. The resistivity of the films was always greater 4.5 x 10^{14} Ω-cm.

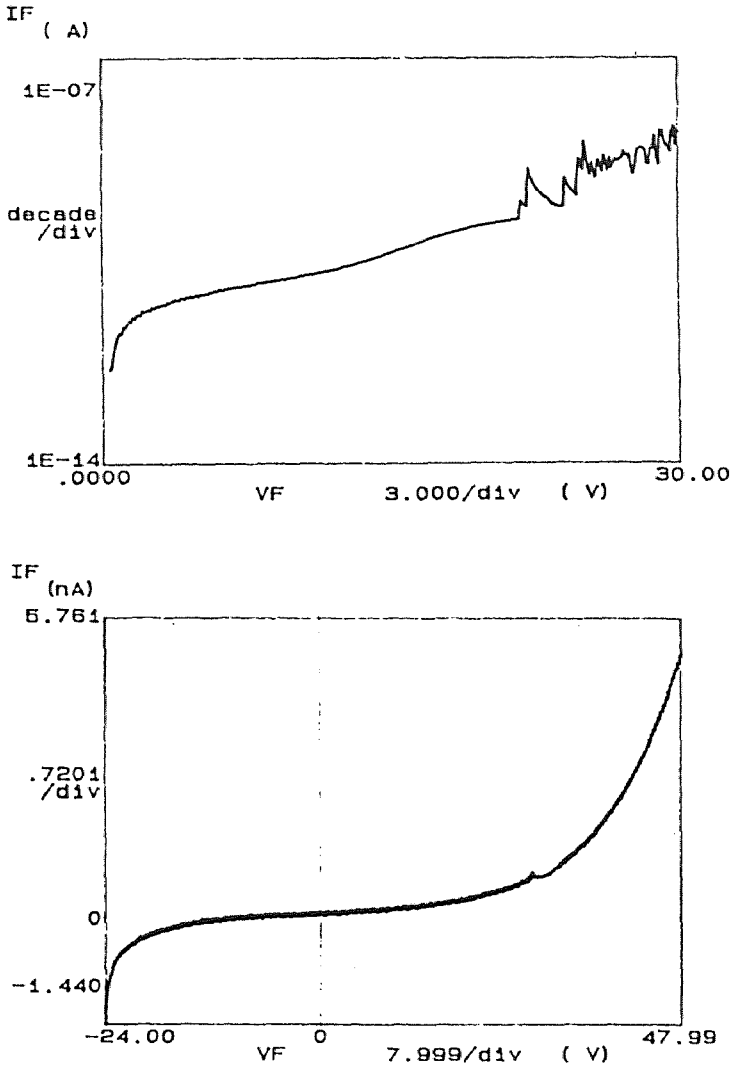

Figure 4.15 I- V characteristics of BN films on (a) type-1 Si and (b) type-2 Si

4.8.4 Capacitance - Voltage Characteristics of the MIS Device upon Illumination

External influences such as temperature, ionization radiation, illumination, and hot carrier injection strongly affect the MOS diode behavior. The motivation for such a study was derived from the fact that modern electronics often involves optical as well as electrical signals. In this particular study, the response of the MIS device to optical generation of EHPs was studied. Fig. 4.16 and Fig. 4.17 show the C-V plots of the device before and after illumination.

The interesting thing about Fig.4.16 is that the BN MIS structures showed deep depletion states when measured using HP-4145B, which had the capability of applying a large positive gate pulse. The deep depletion state in fig 4.16 is represented by the line which tends to have the lowest capacitance at any voltage.

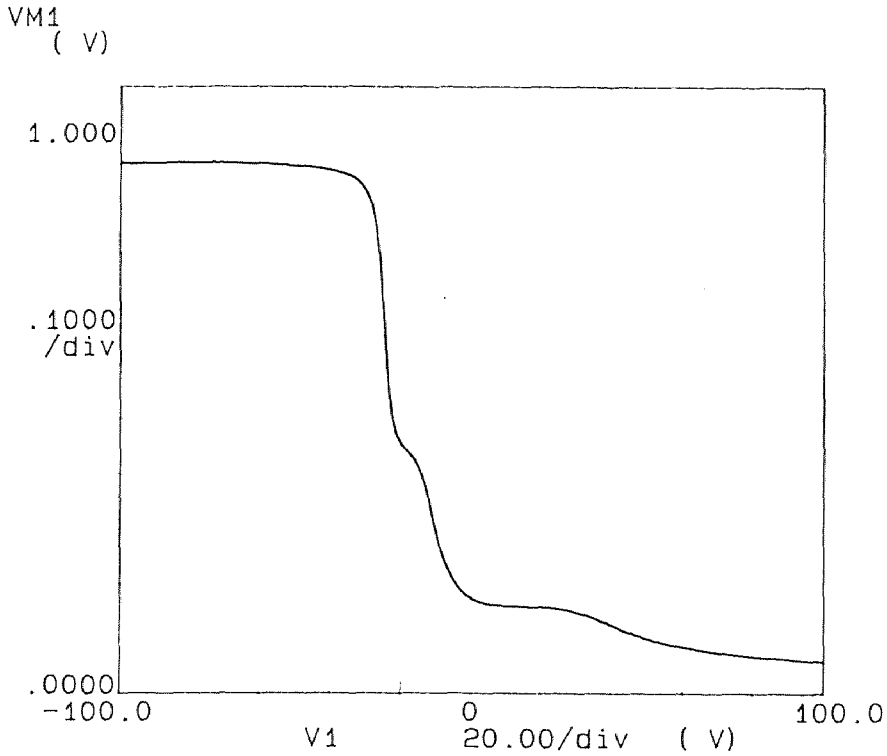

Figure 4.16 C-V characteristic of BN MIS device without illumination (f=1MHz)

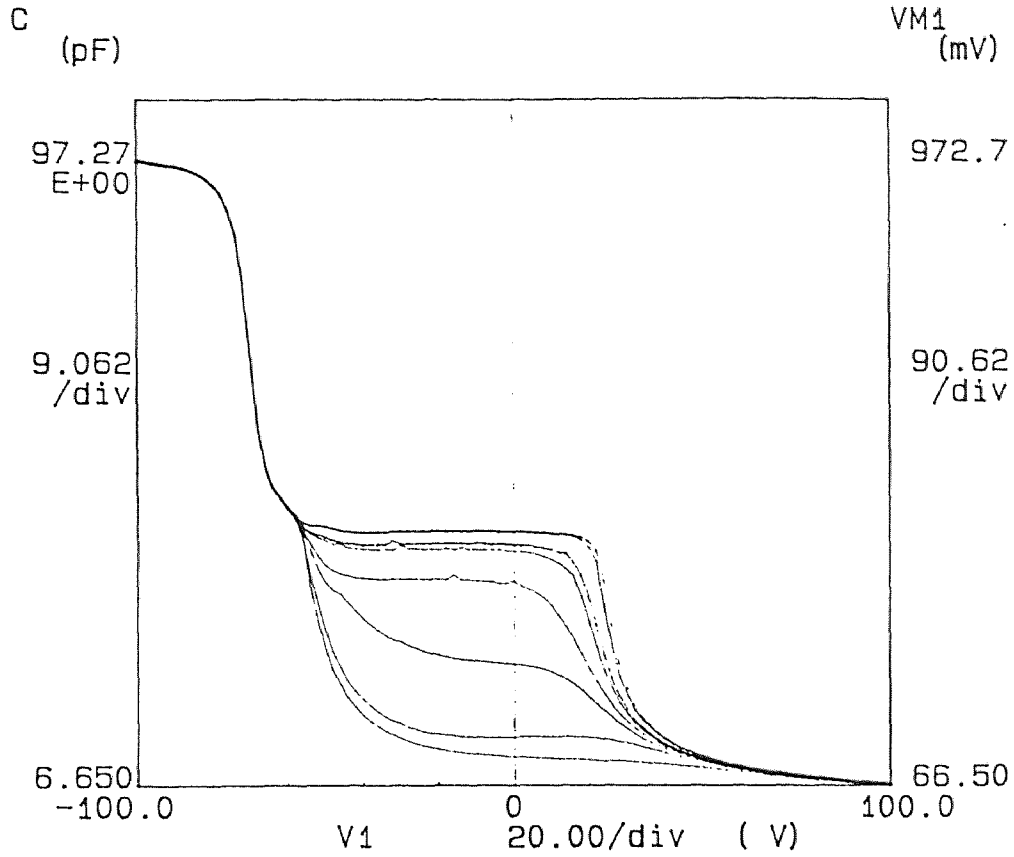

Figure 4.17 Influence of light on the C-V characteristic of BN MIS device (f=1MHz)

From the Fig. 4.16 and 4.17, it was found that their could be a formation of a potential well. This was confirmed by the fact that on photo-illuminating the device with different intensities of light, the device showed the property of charge storage. This kind of behavior of the MIS structure could very well lead to the usage of the boron nitride thin films in the interesting and broadly useful integrated devices known as the charged coupled devices.

CHAPTER 5

CONCLUSIONS

Boron nitride thin films were deposited in a hot walled, horizontal tube low-pressure chemical vapor deposition system using Triethylamine-borane complex and Ammonia as the precursors. Films deposited with a 50:1 Ammonia/TEAB ratio or higher were highly stable and nearly stoichiometric. The deposited films were amorphous, uniform and boron rich at lower temperatures, but with increasing temperature, the films attained compositions close to stoichiometric BN. The refractive index measurements could be questioned due to the presence of about 8% carbon in the elemental form in the film. It was found that the stress on the films were either mildly tensile or compressive (+100Mpa - -150Mpa) depending on the deposition conditions. At higher flow rates the films tended to be stoichiometric and transparent.

Detailed C-V analyses of BN films deposited as MIS structures with p-type substrate were performed. The low frequency (100KHz) curves did not rise back to the C_{ox} levels, representing a threshold voltage shift of more than 30 V. This data can be explained by the presence of a shallow p+ layer at the BN/p-substrate interface. This interpretation is consistent with the suggestion that boron from LPCVD BN diffused into the substrate, forming a p+p junction with a p-type substrate. The formation of the shallow junction could explain the reason for the widely varying values of dielectric constant of BN ranging from 2.7 to 7.7 that have been reported by many researches. Boron rich nitride layer formed during the transient period and subsequent boron diffusion into the silicon substrate probably forms the interface junction

The static dielectric constant values varied from 3.5 to 4.5 depending on the deposition conditions. The optical and the static dielectric constant behavior were similar. The presence of the mobile charge carriers in the films as well as at the substrate-film interface could be one of the reasons for not having achieved lower dielectric constant values. One of the main constraints is the accurate evaluation of the film thickness. Thickness should be measured by some other techniques, probably Tencor/SEM. Also films with lower amount of carbon may give lower dielectric constants. Further study can be done by the addition of Si and forming a ternary film that would be more stable because of the Si-O bonding.

On studying the dynamic effects in the MIS capacitors formed by the BN films, it was seen that on applying a large positive gate pulse, a depletion region existed under the gate, and the surface potential increased considerably under the gate electrode. In effect, the surface potential forms a potential well, which can be exploited for the storage of charge, i.e., before inversion can occur by thermal generation, the depletion width would be greater than it would be at equilibrium. This transient condition is referred to as deep depletion. Further research should be done to find out the capacity of the well for storing charge and the time required to fill the potential well thermally. If the thermal relaxation time of Si with BN film as the insulator turns out to be longer than the charge storage times in the CCD operation time then the boron nitride films could be used as the material for the manufacture of the devices which would find applications in memories, logic functions, signal processing, and imaging.

BIBLIOGRAPHY

1. M.J. Rand and J.F. Roberts, *J. Electrochem.* Soc., **15**, 423 (1968).

2. L.G. Carpenter and P.J. Kirby, *J. Phys.* D, **15**, 1143 (1982).

3. A. Simpson and A.D. Stuckes, *J. Phys.* C, **4**, 1710 (1971).

4 M. Hirayama and K. Shohno, *J. Electrochem. Soc.*, **122**,1671 (1975).

5 T.M. Duncan, R. A. Levy, *J. Appl. Phys.* **64**(6), 15 September 1988.

6 Robert T. Paine and Chaitanya k. Narula, *Chemical Reviews*, 1990, **90**, 1.

7 S.P. Murarka, *Solid State Technology*, March 1996.

8 David Charles, S. Wong, *IEEE Transactions on Elect. Devices*, **39**, 4, 1992.

9 S.P. Murarka, C.C. Chang, D.N.K. Wang and T.E. Smith, *J. Electrochem.Soc.*, **126**, 1951 (1979).

10 M. Hirayama and K. Shohno, *J. Electrochem. Soc.*, **122**,1671 (1975).

11 Francis S. Galasso, *Chemical Vapor Deposited Materials,* CRC publishers, MI, 1984.

12 W. Baronian, *Mat. Res. Bull.*, 7,119 (1972).

13 M Sano, *Thin Solid Films*, **83**, 247 (1981).

14 S Motojima, Y. Tamura and A. Sugiyama, *Thin Solid Films*, **88**, 269 (1982).

15 T. Takahashi, H. Itoh and A. Takeuchi, *J. Crystal Growth*, **47**, 245 (1979).

16 T. Takahashi, H. Itoh and M. Kuroda, *J. Crystal Growth*, **53**,1981 (1981).

17 K. Nakamura, *J. Electrochem. Soc.*,**132**, 1757 (1985).

18 S.S. Dana and J.R. Maldonado, *J. Vac. Sci. Technol.*, **B4**, 235 (1986).

19 A.C. Adams, *J. Electrochem. Soc.*, **128**, 1378 (1981).

20 A.C. Adams and C.D. Capio, *J. Electrochem. Soc.*, **127**, 399 (1980).

21 S.B. Hyber and T.O. Yep, *J. Electrochem. Soc.*, **123**, 1721 (1976).

22 O. Gafri, A. Grill and D. Itzhak, *Thin Solid Films*, **72**,523 (1980).

23 W. Schomolla and H.L. Hartnagel, *J. Appl. Phys.*, **15**,L95 (1982).

24 W. Schomolla and H.L. Hartnagel, *Solid State Electronics*, **26**, 931 (1983).

25 A.J. Noreika, and M.H. Francombe, *Thin Solid Films*, **101**, 722 (1983).

26 M.D. Wiggins and C.R. Aita, *J. Vac. Sci. Technol.* **A2**, 322 (1984).

27 E.H. Lee and H. Poppa, *J. Vac. Sci. Technol.*, **14**, 223 (1977).

28 Weissmantel, K. Bewilogua, K. Breuer, D. Dietrich, U. Ebersbach, H.J. Erler, V. Rao and G. Reisse, *Thin Solid Films*, **96**, 31 (1982).

29 Weissmantel, *J. Vac. Sci. Technol.*, **18**, 2082 (1981).

30 S. Shanfield and R. Wolfson, *J. Vac. Sci. Technol.*, **A1**, 323 (1983).

31 M. Satou and F. Fujimoto, *J. Appl. Phys.*, **22**, L171 (1983).

32 L. Guzman, F. Marchetti, I. Scotoni and F. Ferrari, *Thin Solid Films*, **117**, L63 (1984).

33 M. Sokolowski, A. Sokolowska, A. Michlski, Z. Romanowski, A.R. Mazurek and M.Wronikowski, *Thin Solid Films*, **80**, 249 (1981).

34 M. Maeda and T. Makino, Japan. *J. Appl. Phys.*, **26**, 660 (1987).

35 W.A. Johnson, R.A. Levy, D.J. Resnic, T.E. Saunders, A.W. Yanof, H. Oertel, H. Huber, and , *J. Vac. Sci. Technol.* **B5**, 257 (1987).

36 R.A. Levy, D.J. Resnic, R.C. Frye, A.W. Yanof, G.M. Wells and F. Cerina, *J. Vac. Sci. Technol.*, **B6**, 154 (1988).

37 Maydan, G.A. Coquin, H.J. Levinstein, A.K. Sinha, and D.N.K. Wang, *J. Vac. Sci. Technol.* **16**, 1959 (1979).

38 R.E. Acosta, J.R. Maldonado and R. Fair, *J. Vac. Sci. Technol.* **B4**, 240 (1986).

39 R.K.Laxman, *Semicond. Int.*, 5, 71 (1995).

40 S.V. Nguyen, A. Nguyen, H. Treichel and O. Spindler, *J. Electrochem. Soc.*, **141**, 1635 (1994).

41 T. Usami, K. Shimokawa and M. Yoshimaru, *J. Appl. Phys.*, **33**, 408 (1994).

42. W.P. Kuo, "Synthesis and Characterization of LPCVD Boron Nitride Films for X-ray Lithography, *MS Thesis*, Department of Chemical Engineering, New Jersey Institute of Technology, Newark, NJ (1993).

43. Advanced Semiconductor Materials America, Inc., "Micro 3 Manual".

44. R.A. Levy, E. Mastromatteo, J.M. Grow, V. Paturi and W.P. Kuo, *J. of Mater. Res.*, **10**, 320 (1995).

45. R.A. Levy, *Microelectronic Materials and Processes*, Kluwer Academic Publishers, MA, 1989.

46. Neil H. Hendricks, *Solid State Technology*, July 1995.

47. Keiichiro Kata, Yuzo Shimada and Hideo Takamizawa, *IEEE Trans. on Components, hybrids, and manufacturing technology*, **13**, 2, June 1990.

48. M. Hatanaka, Y. Mizushima, O. Hataishi and Y. Furumura, *Proc. VLSI Multilevel Interconnection Conf.*, 435 (1991).

49. B.L. Chin and E.P. Van de Ven, *Solid State Technol.*, **31**, 119 (1988).

50. Yu, D. Favreau, E. Martin and A. Manocha, *Proc. VLSI Multilevel Interconnect-ion Conf.*, 166 (1990).

51. S. Mizuno, A. Verma, P. Lee and B. Nguyen, *Int. Conf. On Metallurgical Coatings and Thin Films Abstract* (1995)

52. D.C. Rich, P. Cebe and A.K. St.Clair, *Mat. Res. Soc. Symp. Proc.* **323**, 301 (1994).

53. Y. Negi, Y. Suzuki, I. Kawamura, T. Hagiwara, Y. Takahashi, M. Ijima, Y. Imai and M. Kakimoto, *J. Polym. Sci.* **A30**, 2281 (1992).

54. M. Maeda, Japan. *J. Appl. Phys.*, **29** 1789 (1990).

55. M. Maeda, T. Makino, E. Yamamoto and S. Konaka, *IEEE Trans. Electron Devices*, **36**, 1610 (1989).

56. V. Paturi, "Synthesis and Characterization of BN Thin Films for X-ray Masks", *MS Thesis*, Department of Electrical Engineering, New Jersey Institute of Technology, Newark, NJ (1991).

57. M. J. Paisley, L. P. Bourget and R. F. Davis, *Thin Solid Films*, **235** (1993), 30-34.

58. Tue Nguyen, Son Van Nyugen, and David M. Dubuzinsky, *Appl. Phys. Lett.* **63** (15), 11 October 1993.